Supplementary Appendix

This appendix has been provided by the authors to give readers additional information about their work.

Supplement to: Christopher MJ, Petti AA, Rettig MP, et al. Immune escape of relapsed AML cells after allogeneic transplantation. N Engl J Med 2018;379:2330-41. DOI: 10.1056/NEJMoa1808777

Table of Contents

Supplementary Results

Exon sequencing of extramedullary relapse

Extramedullary relapse occurs more commonly after hematopoietic stem cell transplant than after chemotherapy or at presentation.[1-3] This may be due in part to differences in immune surveillance in extramedullary sites, and in fact has been associated with deletion of genes encoding MHC class I.[4] We hypothesized that extramedullary relapse of AML may be associated with mutations involving genes important for immune surveillance or AML cell trafficking. We observed 136 somatic mutations in 6 cases of extramedullary relapse. None occurred in more than a single case and none were in genes that had known immune function, including MHC class I or class II genes (Figure S1). We performed an analysis of the pathways of genes with mutations in extramedullary relapse and bone marrow relapse, and we observed no significant enrichment for cell adhesion or trafficking pathways (data not shown). Given our small sample, however, we cannot rule out that the observed mutations may contribute to extramedullary relapse through unknown mechanisms.

Analysis of putative neoantigens

Loss of cancer-associated neoantigens has also been proposed as a mechanism of immune escape.[5,6] Using a previously published bioinformatic approach[7], we identified potential neoantigens in presentation and relapse samples from patients whose HLA typing was available (n=8 patients). An average of 6.6 possible neoantigens were identified per sample (range 3-13), most of which were present in both presentation and relapse samples. Four patients had possible neoantigens that were cleared at relapse (mean 1.5 per case, range 1-2, Figure S11, Table S9), significantly fewer than have been reported for solid tumors.[6,7] Whether the clearance of these particular variants contributed to relapse in these cases will require further study.

CIITA downregulation and promoter methylation

The coordinate downregulation of MHC class II gene RNA in post-transplant relapse cases raised the possibility they may be regulated by a single master regulatory gene or pathway. A potential candidate is *CIITA,* a transcriptional transactivator that has long been known to play a key role in activating the expression of MHC class II genes.[8,9] Expression of *CIITA* was decreased in 4/6 cases with decreased MHC class II expression (Figure 1). In this subset of cases, *CIITA* expression correlated with MHC class II expression, raising the possibility that in some instances, MHC class II downregulation may be mediated via *CIITA* downregulation (Figure S12C). *CIITA* is not known to affect the expression of many of the other genes that were dysregulated in post-transplant relapses, so other mechanisms are likely relevant for many of these events.

Since *CIITA* silencing has been associated with increased methylation of its promoter region,[10] we performed whole genome bisulfite sequencing on presentation and relapse samples from 3 post-transplant and 3 post-chemotherapy relapse samples (both the post-chemotherapy and post-transplant relapses were evaluated in one patient). Two of the three post-transplant relapse samples had decreased MHC class II expression and the remaining samples had similar expression at presentation as at relapse. Although 1196 differentially methylated regions were identified when comparing the presentation and post-transplant samples (Table S10), virtually none were consistently dysregulated and unique to the post-transplant setting. No MHC class II gene loci were among these regions, and there was no correlation between DNA methylation at MHC class II gene loci and MHC class II mRNA expression (data not shown). However, increased DNA methylation was observed in the region of the *CIITA* promotor/intron 1 in the two post-transplant samples with decreased *CIITA* (and MHC class II) expression (cases 142074 and 452198), but not the samples with unchanged MHC class II mRNA expression (Figure S12A). While preliminary, these data raise the possibility that in some cases, decreased

CIITA expression and subsequent downregulation of MHC class II genes may be related to increased methylation of the *CIITA* promotor/intron 1 region.

Supplementary Methods

Enhanced Exome Sequencing

Sequence data were aligned to reference sequence build GRCh37-lite-build37 using bwa version 0.5.9[11] (parameters: -t = 4, -q = 5), then merged and deduplicated using picard version 1.46[12].

Somatic SNVs were detected using a combination of Samtools, Sniper, Varscan, and Strelka. First, we took the intersection of Samtools version r963[12] (parameters: -A -B; filter: V1), and SomaticSniper version 1.0.2[13] (parameters: -F vcf -q 1 -Q 15; filters: false-positive-filter v1 (parameters: --bam-readcount-version 0.4, –bam-readcount-min-base-quality 15), somatic-score-mapping-quality v1 (parameters: –min-mapping-quality 40 –min-somatic-score 40)). Second, we took the union of VarScan version 2.2.6[14] (filters: varscan-high-confidence filter version v1, false-positive filter v1 (parameters: --bam-readcount-version 0.4 --bam-readcount-min-base-quality 15)), and Strelka version 0.4.6.2[15] (parameters: isSkipDepthFilters = 1). Finally, we took the union of (1) the combined Samtools-and-Sniper output and (2) the combined Varscan-and-Strelka output.

Somatic indels were obtained from the union of the output of 4 methods: (1) GATK somatic-indel version 5336[16,] filtered using false-indel version v1 (parameters: --bam-readcount-version 0.4 --bam-readcount-min-base-quality 15), (2) Pindel version 0.5[17], filtered with pindel-somatic-calls v1, pindel-vaf-filter v1 (parameters: --variant-freq-cutoff 0.08), and pindel-read-support v1, (3) VarScan version 2.2.6[14], filtered with varscan-high-confidence-indel version v1, then with false-indel version v1 (parameters: --bam-readcount-version 0.4 --bam-readcount-min-base-quality 15), and (4) Strelka version 0.4.6.2[15] (parameters: isSkipDepthFilters = 1).

Copy number analysis was performed using VarScan2[14]. Loss of heterozygosity (LOH) was identified using Varscan. Regions with at least 10 contiguous probes and at least 95% LOH were considered to have undergone LOH.

Validation sequencing

Sequence data were aligned to reference sequence build GRCh37-lite-build37 using bwa version 0.5.9[11] (parameters: -t = 4, -q = 5), merged using picard version 1.46[2,] and deduplicated using picard version 1.46 api v2.

Somatic SNVs were obtained from the union of the output of Varscan and Strelka. Varscan v2.2.6 (parameters: --min-var-freq 0.08 --p-value 0.10 --somatic-p-value 0.01 --validation) output was filtered with the varscan-high-confidence filter v1 and the false-positive filter v1 (parameters: --bam-readcount-min-base-quality 15 --bam-readcount-version 0.6).

Indels were detected using four methods, as above, but with updated versions of Strelka (1.0.10) and bam-readcount (0.6).

Variant filtering

Most samples from the post-transplant cohort were sequenced twice. For each of these samples, we considered all variants identified during either the EES or validation sequencing runs, and combined read counts across the runs. We excluded variants that are commonly found in normal samples (based on a large set of in-house sequencing data). Of the remaining variants, we retained those that had a read-depth of at least 30 in all samples from the same patient; had at least 3 variant reads and a VAF ≥ 5 in at least one sample; scored above noise in at least 1 sample according to a binomial test (Code available at https://github.com/genome/genome/blob/master/lib/perl/Genome/Model/Tools/Validation/IdentifyOutliers.pm) (LLR threshold = 10 for 113971 (post-allo relapse sample), 633734 (post-allo relapse sample) and 593890 (all samples), LLR threshold = 3 for all other samples); had an EVS or dbSNP allele frequency below 0.1; and passed manual review of aligned sequence

data. Known AML hotspot mutations (listed in Table S11) were included if they had at least three variant reads and a VAF ≥ 5 in at least one sample, regardless of the other criteria.

The Haplotect algorithm[18] was used to estimate the rate of residual donor contamination in each sorted post-transplant sample. Specifically, the upper limit of the 95% confidence interval of Haplotect's "mle_multi" estimate was used as the estimate of contamination, which in these samples ranged from 4-12%. For each variant that was detected in a given post-transplant sample, but not in the corresponding primary tumor sample, a binomial test was performed to determine whether the VAF was significantly greater than the estimated contamination rate for that sample. Variants were retained if the one-sided *p*-value, adjusted for multiple testing, was at most 0.025.

Mitochondrial mutations and mutations associated with transcript annotation errors were removed. Variants that we believed to represent Clonal Hematopoiesis of Indeterminate Potential (CHIP) were removed. The VAFs of X-chromosome variants in males were corrected by dividing the observed VAF by 2. All samples were manually reviewed to identify *FLT3* internal tandem duplications and *NPM1* insertions (and their corresponding VAFs) that may have been missed by the algorithms above. This resulted in the inclusion of 4 variants: a *FLT3* ITD and an *NPM1* insertion in each of the AMLs 312451 and 327733. Two variants identified using fluorescent *in situ* hybridization (FISH) were also included: an *MLL-ELL* fusion in AML 242129, and a *CBFB-MYH11* fusion in AML 619751.

RNA-seq data analysis

Kallisto v0.43.0[19] was used to quantify transcript abundances (default parameters), using a GRCh37 transcriptome index generated from Ensembl v74 (default parameters). Kallisto's transcript-level abundance estimates were converted into length-scaled, gene-level counts using the R package tximport v1.0.3[20]. EdgeR v3.14.0[21] was used to filter genes based on counts per million (CPM > 1 in at least 10 samples), normalize counts using the TMM

algorithm[22], and identify genes that are differentially expressed between primary and relapse samples. Specifically, 2 separate linear models were fit to the data: the first was fit to the paired primary and post-transplantation relapse samples; the second was fit to the paired primary and post-chemo relapse samples. *p*-values for the fits were obtained using a likelihood ratio test, and false discovery rates (FDRs) were calculated using the Benjamini-Hochberg method. A gene was classified as differentially expressed if its FDR was at most 0.05. These calculations were performed in R v3.3.1. Gene Ontology enrichment was performed using ToppFun[23], which uses a hypergeometric test to determine the significance of the enrichment. The resulting p-value is the probability of obtaining the observed intersection (between a set of differentially expressed genes and the genes in the annotated functional category) by chance. Multiple hypothesis correction in gene set enrichment analysis was done using the Benjamini-Hochberg method for controlling the false discovery rate.

As a quality control for sample purity, variant allele frequency (VAF) of each variant present in RNA sequencing of post-TRANSPLANT and post-chemotherapy cohorts was compared to that variant's VAF as established by previous DNA sequencing. Samples with poor correlation between DNA and RNA were excluded (AML161510, AML242129, AML275291, AML303642, AML763312, AML275291).

Bisulfite sequencing analysis

Bisulfite sequencing reads were mapped with BSMAP (version 2.74)[24] using default parameters, followed by quantification of methylation ratios with the included methratio.py script. Differentially methylated regions between diagnosis and post-transplant samples were called using metilene v.0.2-6.[25]

Flow cytometry

Flow cytometry was performed as previously described.[26] For flow sorting of AML cells, cryovials were thawed in 40% FBS in PBS and stained with the following antibodies: PerCP-

Cy5.5-conjugated anti-human CD45 (eBiosciences, San Diego, CA; clone 2D1), FITC-conjugated anti-human CD19 (BD Pharmingen, Franklin Lakes, NJ; clone HIB19), e450-conjugated anti-human CD3 (eBiosciences, clone OKT3), PE-conjugated anti-human CD34 (Miltenyi, Auburn, CA; PE-pool, PN IM1459U). For MHC Class II analysis, cells were stained with anti-human CD45 and a BV421-conjugated Mouse Anti-Human HLA-DR, DP, DQ antibody (BD Biosciences, San Jose, CA; clone Tu39).

Cell Culture

Culture of primary AML samples was performed as previously described.[27] Briefly, cryovials with primary cells were thawed in PBS containing 30% FBS, centrifuged, resuspended in media with cytokines, and plated on HS27 stromal cells. Cells were cultured with or without interferon gamma (10ng/ml or 50ng/ml, Peprotech, Rocky Hill, NJ) and were analyzed at different time points for MHC Class II expression by flow cytometry as described above.

Mixed lymphocyte reaction

Cryopreserved peripheral blood or bone marrow mononuclear cells from AML patients were thawed, washed, and cultured overnight on human HS27 stromal cells as before. The non-adherent cells were collected, irradiated (3500 cGy), and used as stimulators. Third party (MHC mismatched) CD4+ T lymphocytes were isolated from healthy PBMC donors by negative selection using an AutoMACS device per the manufacturer's instructions (Miltenyi Biotech, Auburn, CA) and used as responders. In the human interferon gamma enzyme linked immunospot (ELISPOT) assay, 3.3×10^4 CD4+ T cells were plated with 1×10^5 stimulator cells in precoated human IFN-γ ELISPOT plates (Cellular Technology Ltd., Shaker Heights, OH) containing 200 ul of serum-free Stemline T cell expansion medium (Sigma-Aldrich, St. Louis, MO) supplemented with 1% GlutaMax (Life Technologies, Invitrogen, Waltham, Massachusetts) and 1% Corning Cellgro penicillin-streptomycin solution (Mediatech, Manassas, Virginia). Stimulation of CD4+ T cells with phorbol 12-myristate 13-acetate (PMA; 5 ng/mL) and ionomycin (1 ng/ml; Sigma-Aldrich, St. Louis, Missouri) was used as a positive control. Triplicate

wells of T cells or AML stimulators alone were used as the background control. Plates were incubated at 37°C for 36 hours and analyzed by C.T.L. ImmunoSpot kit and ImmunoSpot S6 analyzer (Cellular Technology Ltd., Shaker Heights, OH). In parallel, flow cytometric analysis of separate MLR cultures was performed to determine the percentage of CD4+ T cells that became activated in response to allo-stimulation. Here, 2 x 10^5 CD4+ T cells were plated with 2 x 10^5 stimulator cells in 96-well round bottom plates containing 200 ul of serum-free Stemline T cell expansion medium supplemented with 10% human AB serum, 1% GlutaMax, and 1% Corning Cellgro penicillin-streptomycin solution. Stimulation of CD4+ T cells with Dynabeads human T activator CD3/CD28 beads (1 bead per cell; Thermo Fisher Scientific, Waltham, Massachusetts) was used as a positive control and unstimulated T cells were used as the background control. Plates were incubated at 37°C for 4 to 5 days. Cells were then harvested, resuspended in staining buffer (PBS supplemented with 0.5% bovine serum albumin and 2 mM EDTA) and incubated for 30 min at 4^o C with pre-titrated saturating dilutions of the following fluorochrome-labeled monoclonal antibodies (BD Biosciences; clone designated in parenthesis): CD3 (UCHT1), CD4 (SK3), CD8 (SK1), CD14 (MPHIP9), CD33 (P67.6), CD34 (581), CD45 (2D1), CD117 (YB5.B8), CD123 (7G3), CD279 (EH12.1), and CD137 (4B4-1). Dead cells were excluded from these assays by staining with 2 ug/ml 7-amino-actinomycin D (Molecular Probes, Eugene, OR) for 5 min prior to analysis. Appropriate isotype-matched negative controls were used to assess background fluorescence intensity and set gates for negative populations. Samples were analyzed on a Gallios flow cytometer (Beckman Coulter, Brea, California) and data were analyzed using FlowJo software (TreeStar, Ashland, OR). The percentage of viable CD45+/CD3+/CD4+/CD137+/CD279+ T cells within the entire CD45+/CD3+/CD4+/CD8-/CD14-/CD33-/CD34-/CD117-/CD123- subset was quantified.

Single cell RNA sequencing:

We used the Chromium instrument and the Single Cell 3' Solution from 10x Genomics[28] to generate scRNA-seq data for paired presentation/relapse samples from AML 452198, and whole bone marrow samples from four healthy donors. Briefly, cryopreserved cells were thawed

as described above, viable cells were flow sorted based on propridium iodide exclusion and resuspended in 1X PBS containing 0.04% weight/volume BSA. Aliquots were partitioned using the Chromium instrument into as many as 18,000 nanoliter-scale Gel Bead-in-Emulsions (GEMs). cDNA libraries were prepared from individual GEM-partitioned cells using the Chromium Single Cell 3' Chip Kit v2 (PN-120236), Library & Gel Bead Kit v2 (PN-120237), and Chromium i7 Multiplex Kit (PN-120262), according to the instructions in the ChromiumTM Single Cell 3' Reagent Kits v2 User Guide, Rev A.[28] cDNA libraries were sequenced on the Illumina HiSeq 4000 to a depth of at least 50,000 reads/cell. CellRanger (10x Genomics) and the cellrangerRkit package (10x Genomics) were used to demultiplex and align the sequencing reads, correct and count the UMIs for each gene in each cell, normalize the data to account for differences in sequencing depth across samples, exclude genes with zero UMI counts, normalize read depth across cells within each data set, perform dimensionality reduction, and perform k-means and graph-based clustering. Cell-type inference was performed in an unsupervised, marker-free manner by training a nearest-neighbor algorithm on expression data from the DMAP database,[20] and in a supervised manner used known cell-type markers.

Single cell RNA sequencing read counts.

Sample	Number of Cells	Total Reads/Cell	Reads/Cell Mapped to Transcriptome	Median Genes/Cell	Total genes detected	Median UMI counts per cell
452198 Presentation	18,126	79,616	38,773	1,381	21,342	3,570
452198 Relapse	10,429	141,786	70,752	1,438	21,036	4,144
Normal 1	1,724	291,981	155,626	1,404	20,124	4,728
Normal 2	2,435	172,633	97,538	1,004	18,945	3,210
Normal 3	1,954	404,932	241,340	1,650	19,885	6,815
Normal 4	1,944	396,078	240,420	1,817	19,694	7,614

Supplementary Appendix References

1. Harris AC, Kitko CL, Couriel DR, et al. Extramedullary relapse of acute myeloid leukemia following allogeneic hematopoietic stem cell transplantation: incidence, risk factors and outcomes. Haematologica 2013;98:179-84.
2. Shimizu H, Saitoh T, Hatsumi N, et al. Prevalence of extramedullary relapses is higher after allogeneic stem cell transplantation than after chemotherapy in adult patients with acute myeloid leukemia. Leuk Res 2013;37:1477-81.
3. Simpson DR, Nevill TJ, Shepherd JD, et al. High incidence of extramedullary relapse of AML after busulfan/cyclophosphamide conditioning and allogeneic stem cell transplantation. Bone Marrow Transplant 1998;22:259-64.
4. Stölzel F, Hackmann K, Kuithan F, et al. Clonal Evolution Including Partial Loss of Human Leukocyte Antigen Genes Favoring Extramedullary Acute Myeloid Leukemia Relapse After Matched Related Allogeneic Hematopoietic Stem Cell Transplantation. Transplantation 2012;93:744-9.
5. Anagnostou V, Smith KN, Forde PM, et al. Evolution of Neoantigen Landscape during Immune Checkpoint Blockade in Non-Small Cell Lung Cancer. Cancer Discov 2017;7:264-76.
6. Matsushita H, Vesely MD, Koboldt DC, et al. Cancer exome analysis reveals a T-cell-dependent mechanism of cancer immunoediting. Nature 2012;482:400-4.
7. Hundal J, Carreno BM, Petti AA, et al. pVAC-Seq: A genome-guided in silico approach to identifying tumor neoantigens. Genome Med 2016;8:11.
8. Anderson DA, 3rd, Grajales-Reyes GE, Satpathy AT, Hueichucura CEV, Murphy TL, Murphy KM. Revisiting the specificity of the MHC class II transactivator CIITA in classical murine dendritic cells in vivo. Eur J Immunol 2017.
9. Ting JP, Trowsdale J. Genetic control of MHC class II expression. Cell 2002;109 Suppl:S21-33.
10. Morimoto Y, Toyota M, Satoh A, et al. Inactivation of class II transactivator by DNA methylation and histone deacetylation associated with absence of HLA-DR induction by interferon-gamma in haematopoietic tumour cells. Br J Cancer 2004;90:844-52.
11. Li H, Durbin R. Fast and accurate short read alignment with Burrows-Wheeler transform. Bioinformatics 2009;25:1754-60.
12. Li H, Handsaker B, Wysoker A, et al. The Sequence Alignment/Map format and SAMtools. Bioinformatics 2009;25:2078-9.
13. Larson DE, Harris CC, Chen K, et al. SomaticSniper: identification of somatic point mutations in whole genome sequencing data. Bioinformatics 2012;28:311-7.
14. Koboldt DC, Zhang Q, Larson DE, et al. VarScan 2: somatic mutation and copy number alteration discovery in cancer by exome sequencing. Genome Res 2012;22:568-76.
15. Saunders CT, Wong WS, Swamy S, Becq J, Murray LJ, Cheetham RK. Strelka: accurate somatic small-variant calling from sequenced tumor-normal sample pairs. Bioinformatics 2012;28:1811-7.
16. McKenna A, Hanna M, Banks E, et al. The Genome Analysis Toolkit: a MapReduce framework for analyzing next-generation DNA sequencing data. Genome Res 2010;20:1297-303.
17. Ye K, Schulz MH, Long Q, Apweiler R, Ning Z. Pindel: a pattern growth approach to detect break points of large deletions and medium sized insertions from paired-end short reads. Bioinformatics 2009;25:2865-71.
18. Sehn JK, Spencer DH, Pfeifer JD, et al. Occult Specimen Contamination in Routine Clinical Next-Generation Sequencing Testing. Am J Clin Pathol 2015;144:667-74.
19. Bray NL, Pimentel H, Melsted P, Pachter L. Near-optimal probabilistic RNA-seq quantification. Nat Biotechnol 2016;34:525-7.
20. Soneson C, Love MI, Robinson MD. Differential analyses for RNA-seq: transcript-level estimates improve gene-level inferences. F1000Res 2015;4:1521.
21. Robinson MD, McCarthy DJ, Smyth GK. edgeR: a Bioconductor package for differential expression analysis of digital gene expression data. Bioinformatics 2010;26:139-40.

22. Robinson MD, Oshlack A. A scaling normalization method for differential expression analysis of RNA-seq data. Genome Biol 2010;11:R25.
23. Chen J, Bardes EE, Aronow BJ, Jegga AG. ToppGene Suite for gene list enrichment analysis and candidate gene prioritization. Nucleic Acids Res 2009;37:W305-11.
24. Xi Y, Li W. BSMAP: whole genome bisulfite sequence MAPping program. BMC Bioinformatics 2009;10:232.
25. Juhling F, Kretzmer H, Bernhart SH, Otto C, Stadler PF, Hoffmann S. metilene: fast and sensitive calling of differentially methylated regions from bisulfite sequencing data. Genome Res 2016;26:256-62.
26. Klco JM, Spencer DH, Miller CA, et al. Functional heterogeneity of genetically defined subclones in acute myeloid leukemia. Cancer Cell 2014;25:379-92.
27. Klco JM, Spencer DH, Lamprecht TL, et al. Genomic impact of transient low-dose decitabine treatment on primary AML cells. Blood 2013;121:1633-43.
28. Zheng GX, Terry JM, Belgrader P, et al. Massively parallel digital transcriptional profiling of single cells. Nat Commun 2017;8:14049.

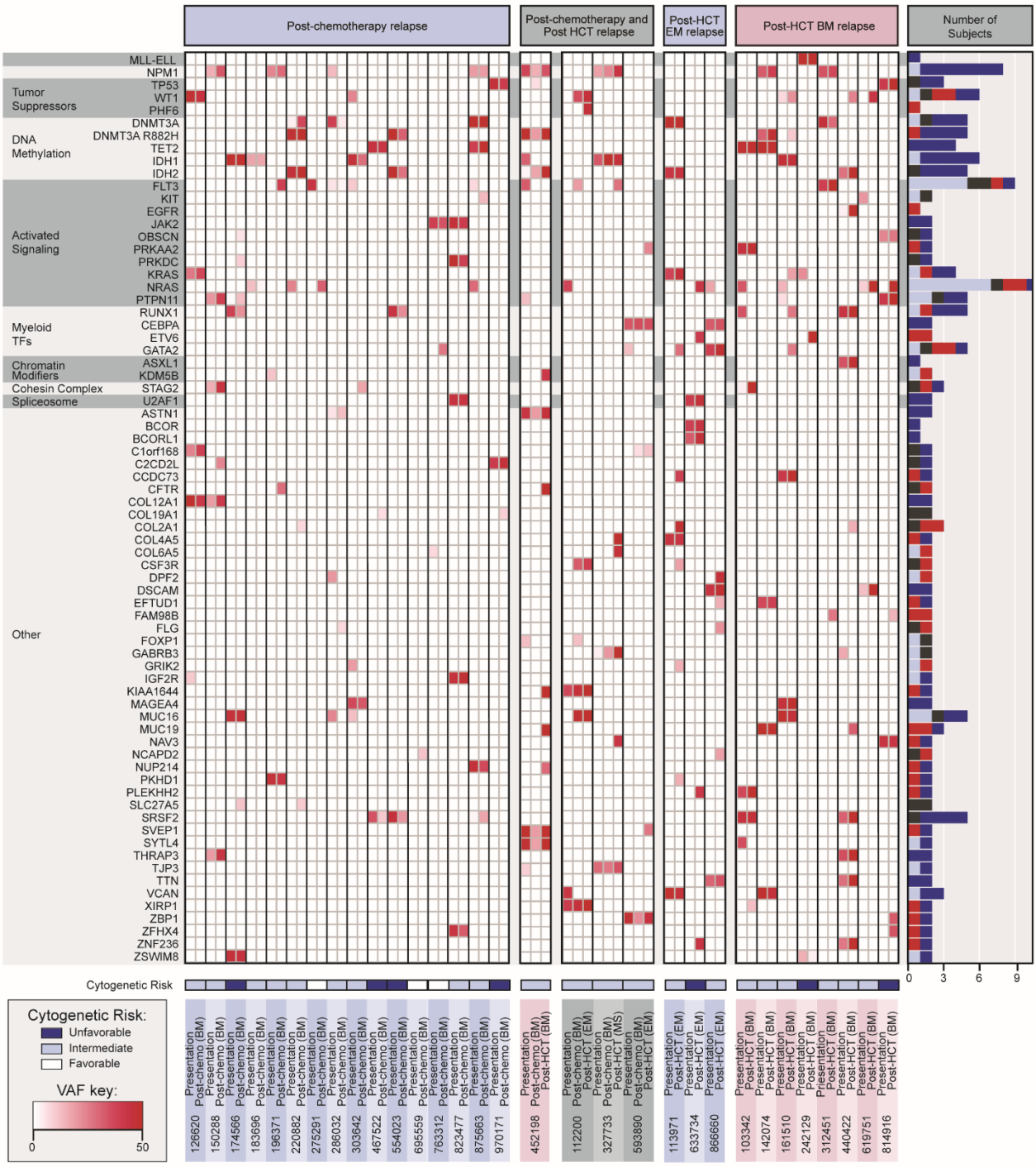

Figure S1. Mutational spectrum of AML relapsing after chemotherapy vs. transplant. Somatic mutations occurring in at least two samples are shown. Each column represents paired presentation/relapse samples and are grouped by the type of relapse (post-chemo, post-hematopoietic stem cell transplant (HCT) bone marrow, or post-transplant myeloid sarcoma [i.e. extramedullary relapse]). Histograms on the right reflect the number of unique patients in whom each gene is mutated in this sample set, as well as when the mutation was detected (presentation sample, post-chemo relapse, post-transplant bone marrow [BM] relapse, post-transplant extramedullary [EM] relapse). Mutations are coded as being detected in the presentation sample (light blue), relapse post-chemo sample (black), relapse post-transplant sample (red), or shared in the presentation and relapse samples (dark blue).

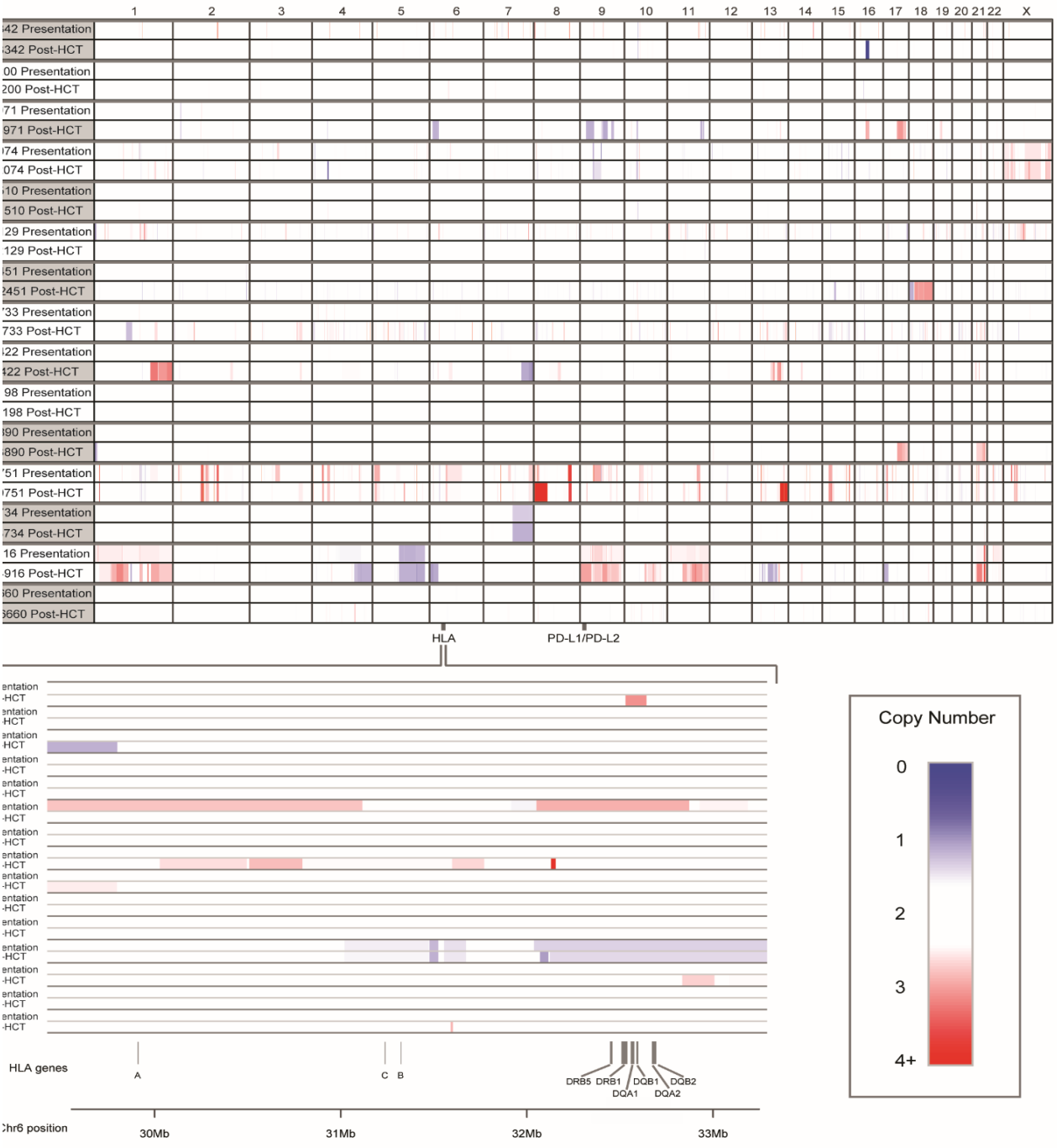

Figure S2: Copy Number Alterations in Post Transplant Cases (A) Copy number changes in matched presentation and post hematopoietic stem cell transplant (post-transplant) relapse samples across the entire genome, by chromosome. Red indicates amplification, blue indicates deletion, and white indicates copy number neutral regions. The inset shows the MHC locus on chromosome 6p21.3. The region encompassing *PD-L1* and *PD-L2* on chromosome 9p24 is also indicated.

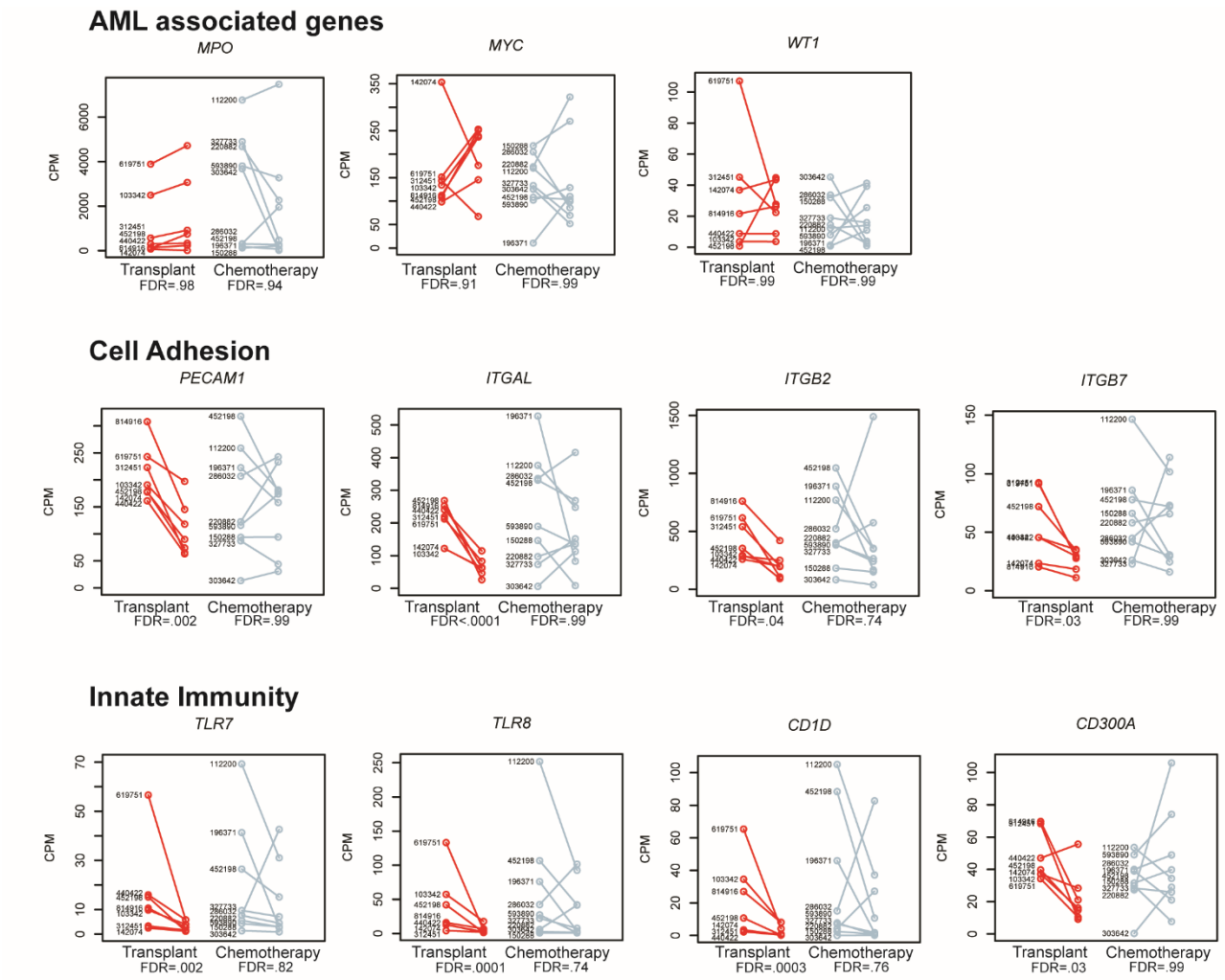

Figure S3: Dysregulated gene expression in AML cells after relapse. RNA sequencing was performed on enriched leukemia blast cells from matched presentation and relapse samples, and differentially expressed genes were identified in post-transplant relapse compared to matched presentation samples based using statistically defined methods. Shown are line plots of representative genes from different functional categories (for complete list of differentially regulated genes, normalized RNA sequencing data, and pathway analysis, see Tables S6-S8) are shown.

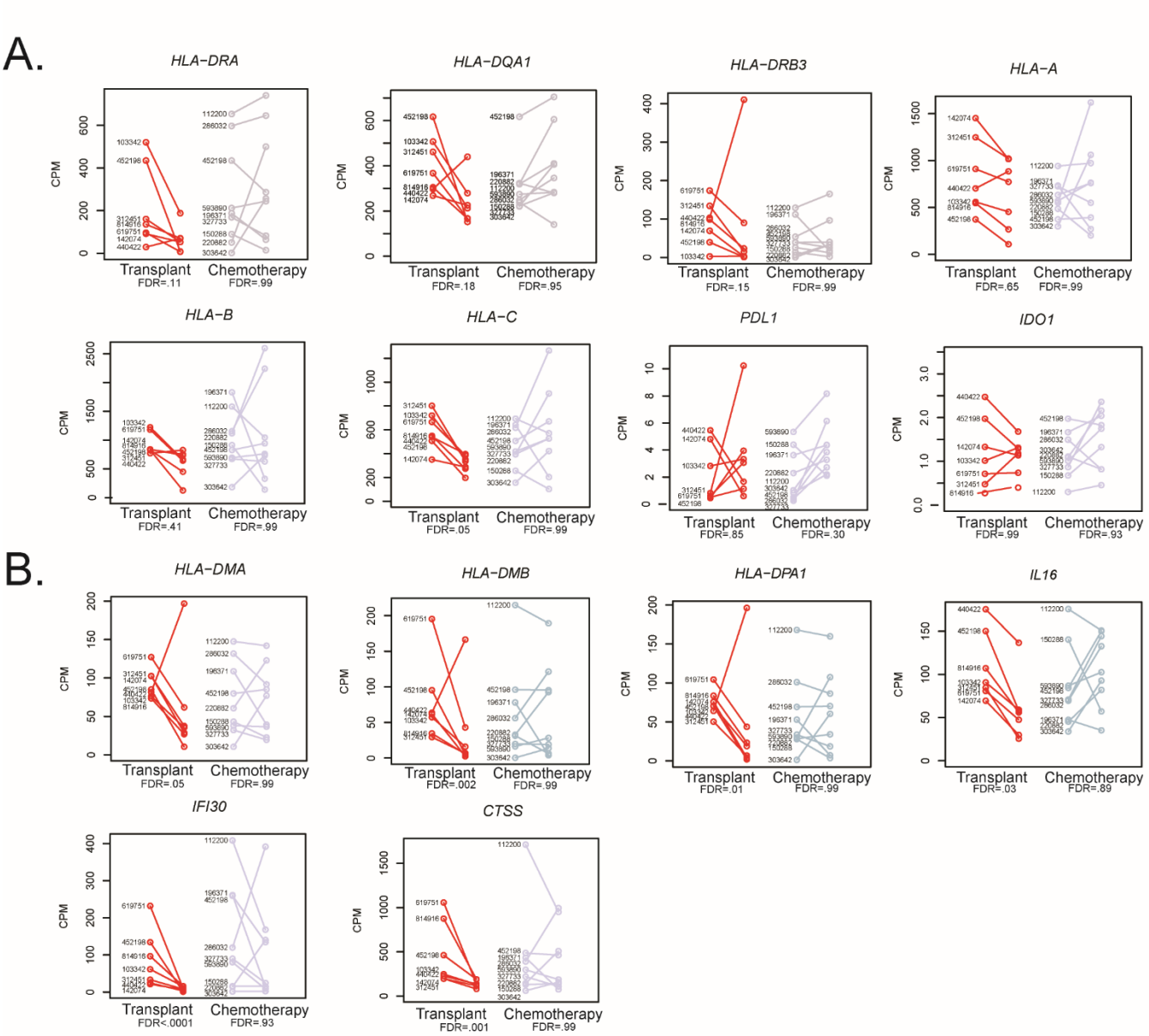

Figure S4: Expression of Immune-Related Genes in AML Cells after Transplant. RNA sequencing, analysis, and plotting is identical to that of Figure 1. (A) MHC class II genes (*HLA-DRA, HLA-DQA1, AND HLA-DRB3*), MHC class I genes, and *PDL1* and *IDO1* expression levels, after post-transplant relapse vs. post-chemotherapy relapse. (B) MHC class II and MHC class II-related genes *HLA-DMA, HLA-DMB, HLA-DPA1, IL16, IFI30*, and *CTSS* were identified as downregulated by predefined criteria in the post-transplant relapse cases, but not in the post-chemotherapy cases.

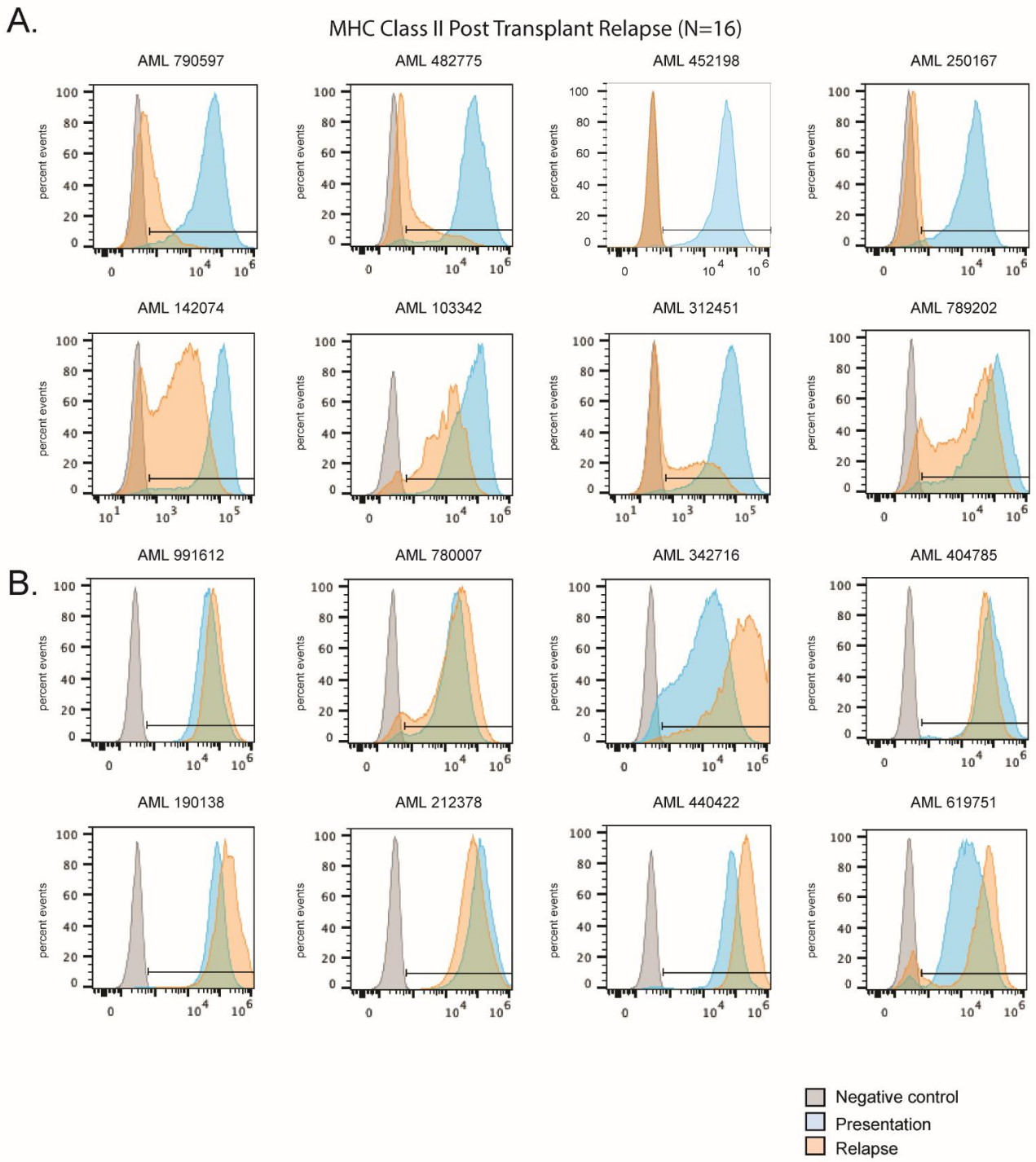

Figure S5: Flow Cytometry for MHC Class II Expression Post-transplant. Cryopreserved presentation/relapse pairs (N=16) were stained with an antibody against HLA-DP,DQ,DR (MHC class II). Shown is MHC class II expression on CD45 dim, side scatter low blasts from diagnosis (blue histograms), relapse (orange histogram), and negative control (grey histogram). (A) 8/16 cases show either substantial (>60-fold decrease, AML312451, AML452198, AML250167, AML482775, AML790597) or partial (4-22 fold decrease, AML103342, AML789202, and AML142074) downregulation of MHC class II expression based on mean fluorescence intensity. (B) The remaining 8 cases showed no decrease in MHC class II expression. X axes show fluorescent intensity on a log scale, Y axes are percent events

normalized to the modes of each sample. Negative controls represent fluorescence-minus-one controls.

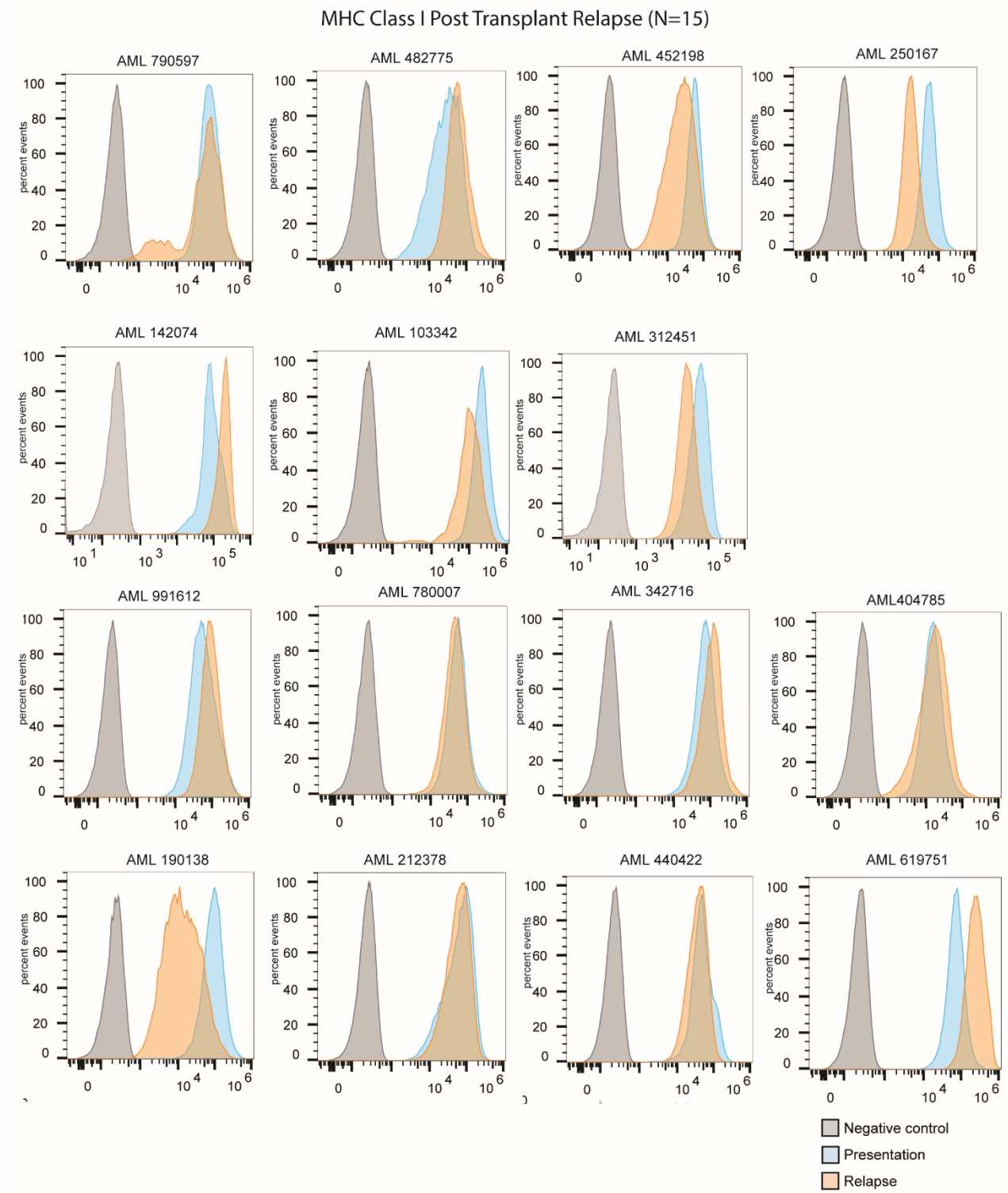

Figure S6: Flow Cytometry for MHC class I Expression Post-transplant. Cryopreserved presentation/relapse pairs (N=15) were stained with an antibody against HLA-A,B,C (MHC class I). Shown is MHC class I expression on CD45 dim, side scatter low blasts from diagnosis (blue histograms), relapse (orange histogram), and isotype control (grey histogram). X axes show fluorescent intensity on a log scale, Y axes are percent events normalized to the modes of each sample. Negative controls represent fluorescence-minus-one controls.

A.

UPN	Diagnosis HLA-DR positive blasts	1st Relapse HLA-DR positive blasts	2nd Relapse HLA-DR positive blasts	HLA-DR DOWNREGULATED
EXT 1	<5%	5-10%	NA	
EXT 2	<5%	5-10%	NA	
EXT 3	<5%	10-20%	NA	
EXT 4	>50%	<5%	NA	yes
EXT 5	20-30%	<5%	NA	yes
EXT 6	20-30%	20-30%	NA	
EXT 7	20-30%	<5%	NA	yes
EXT 8	20-30%	<5%	NA	yes
EXT 9	30-40%	<5%	NA	yes
EXT 10	30-40%	30-40%	NA	
EXT 11	30-40%	5-10%	NA	yes
EXT 12	30-40%	<5%	NA	yes
EXT 13	5-10%	>50%	NA	
EXT 14	5-10%	<5%	NA	
EXT 15	5-10%	10-20%	NA	
EXT 16	20-30%	10-20%	<5%	yes
EXT 17	10-20%	10-20%	NA	
EXT 18	10-20%	<5%	NA	yes

B.

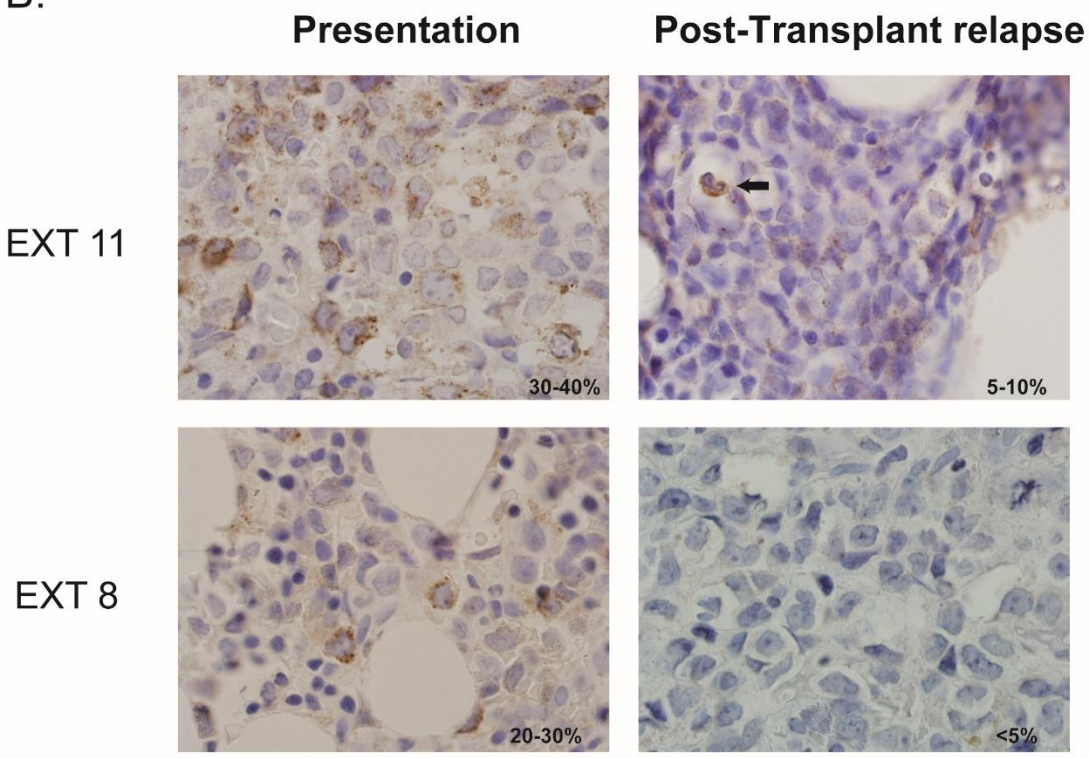

Figure S7: Immunohistochemistry for HLA-DR Post-Transplant. (A) 18 patients had detectable HLA-DR protein. 9/18 patients had decrease in HLA-DR staining at relapse, and 8 of these had <5% blasts staining HLA-DR positive. (B) H&E stained photomicrographs showing regions of AML involvement in presentation and relapse biopsies from two representative cases from the immunohistochemistry cases, EXT11 and EXT8. Brown cytoplasmic stain is HLA-DR protein. Arrow indicates mature neutrophil staining positive for HLA-DR amid HLA-DR negative blasts.

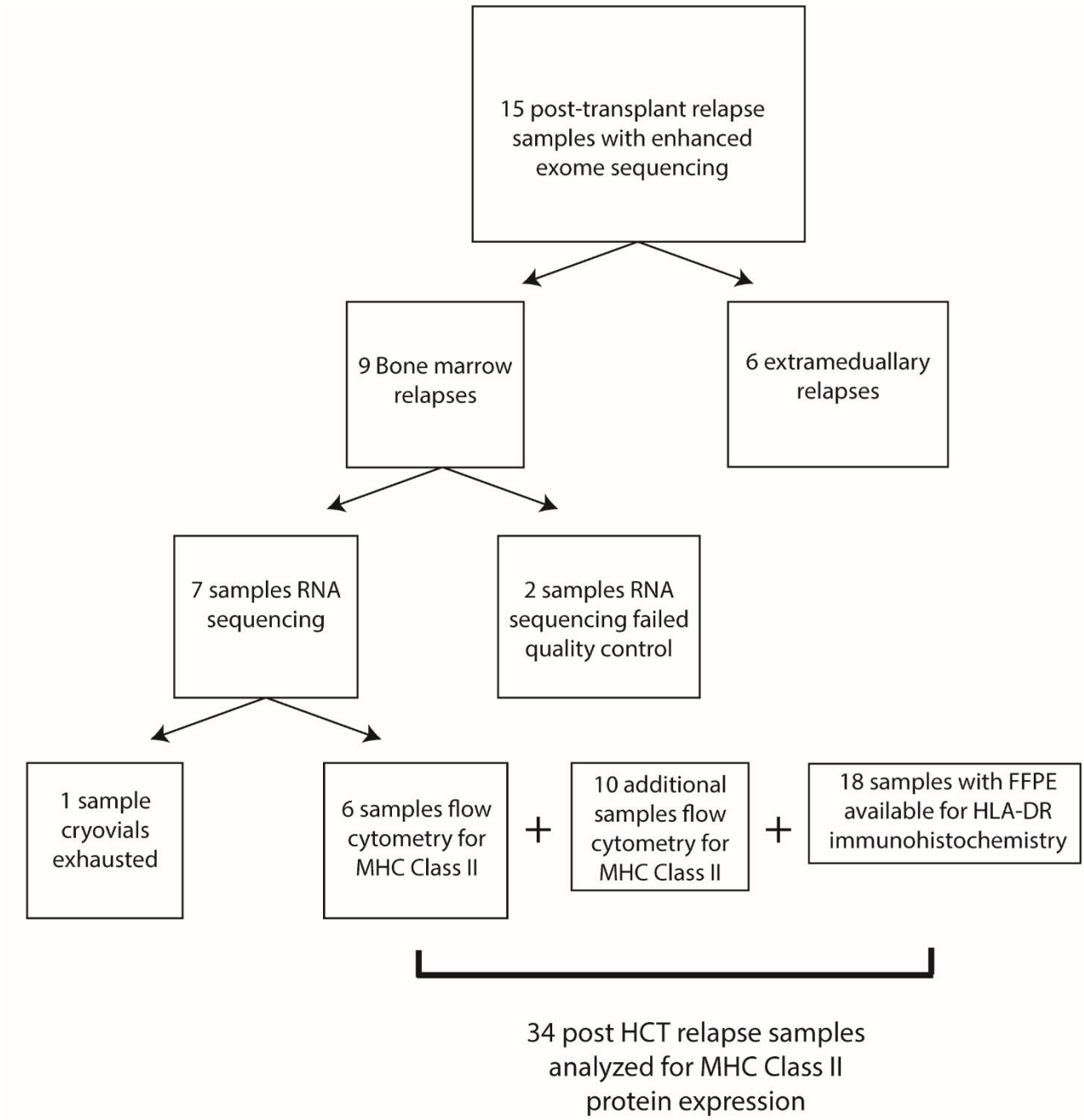

Figure S8. Flow chart showing samples analyzed for MHC class II expression. 15 samples were analyzed by enhanced exome sequencing. Of these 9 samples had bone marrow relapses with available cryovials for RNA sequencing analysis. 2 of these failed QC measures (see Supplementary Methods section) and the remaining 7 were analyzed for differential gene expression analysis, revealing downregulation of MHC class II genes (Figure 1 and Figure S4B). To validate these findings, 6 samples were analyzed by flow cytometry (one sample had no further cryovials available). An additional 10 post-transplant cases with presentation and relapse samples were analyzed by flow cytometry for MHC class II (Figure S5). Finally, 18 samples were identified with FFPE bone marrow cores from post-transplant relapses and HLA-DR immunohistochemistry was performed on these. Clinical data on all patients is found in Table S1-S2.

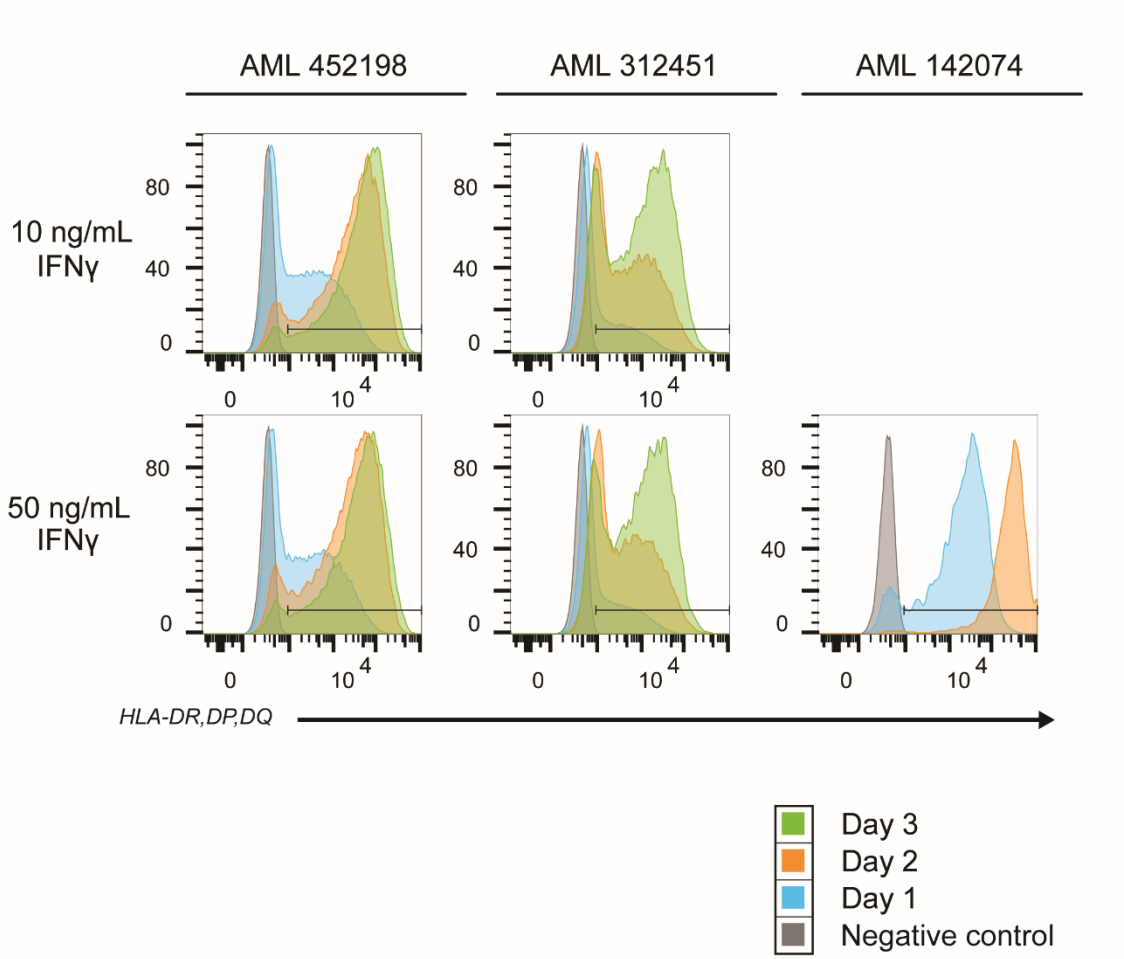

Figure S9: Induction of MHC Class II Expression with Interferon Gamma. Cryopreserved leukemia cells from 3 post-transplant relapse samples with downregulated MHC class II expression were cultured for up to 72 hours in the presence or absence of IFNγ, 10ng/ml (top panels) or 50ng/ml (bottom panels). MHC class II expression in the blast population was assessed by flow cytometry at different time points, as indicated. Negative controls represent fluorescence-minus-one controls.

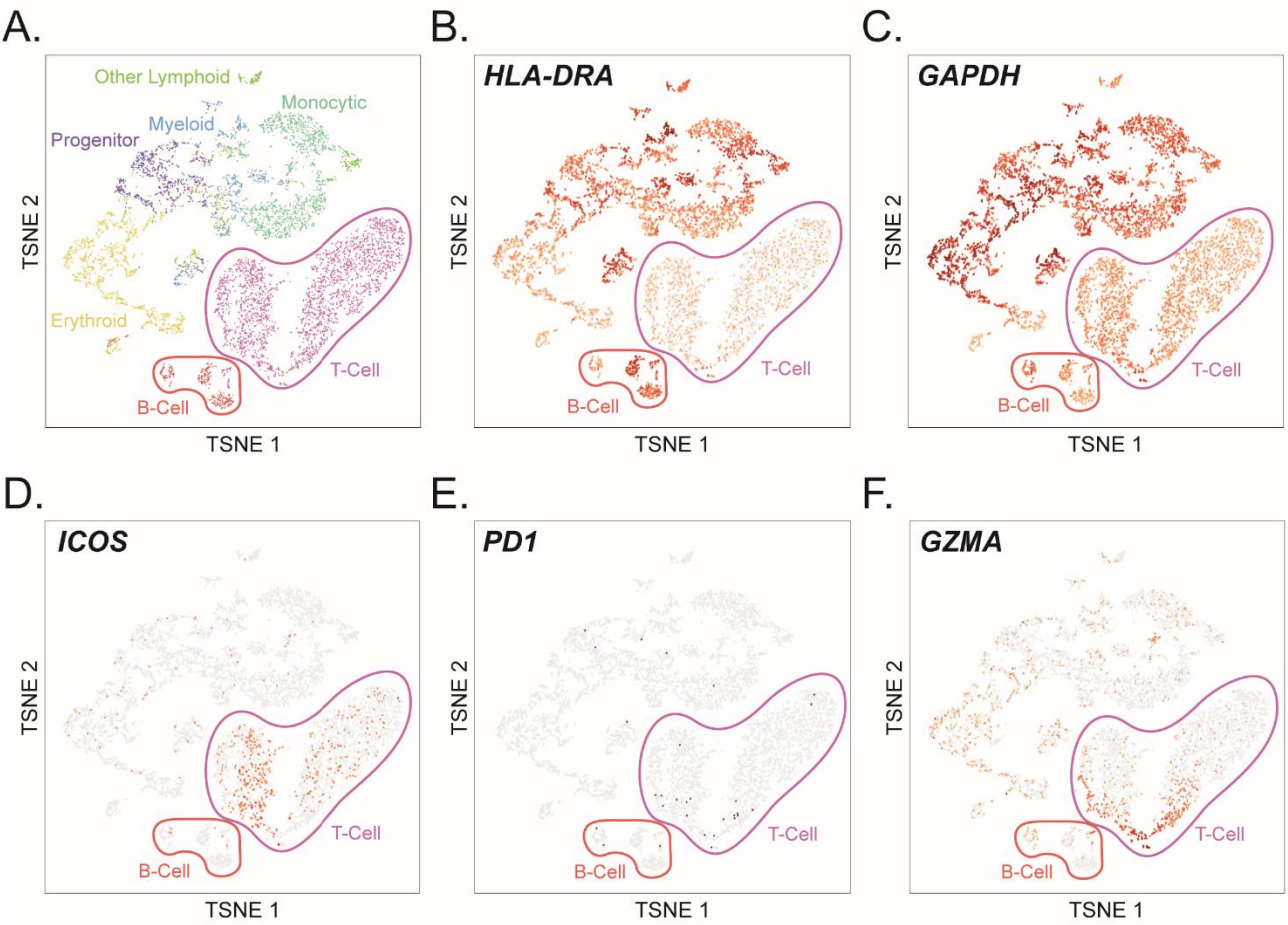

Figure S10: Single-cell RNA Sequencing of Normal Bone Marrow. Single-cell RNA sequencing was performed on cryopreserved normal bone marrows from healthy adult individuals (N=4). Cells from all 4 samples were superimposed on a single 2D plot and clustered based on their unique expression profiles using t-distributed stochastic neighbor embedding (t-SNE). (A) t-SNE plot of normal bone marrow cells with pseudo-coloring of cells based on RNA expression, and identification of the lineages of each population. Cell populations from different samples cluster together. (B-F) Color intensity shows expression of the indicated gene within each population.

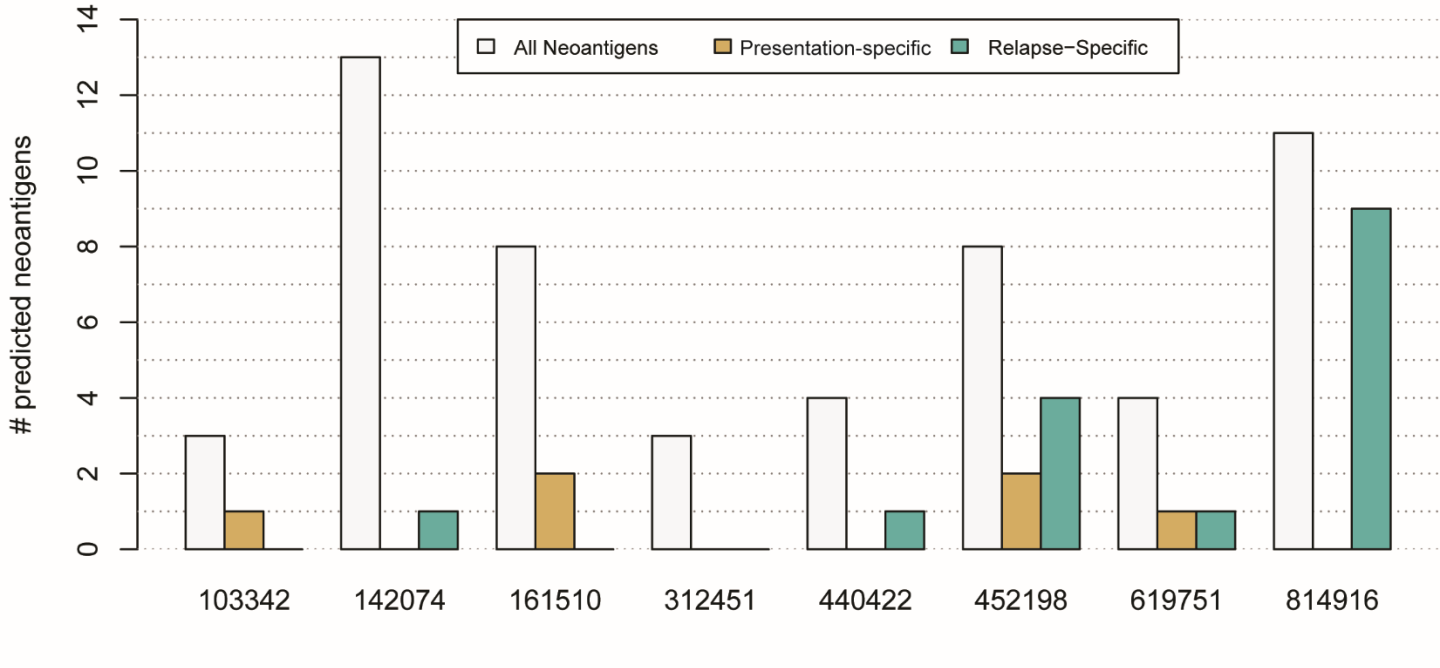

Figure S11: Bioinformatic Analysis of Putative Neoantigens at Presentation and Relapse. Expressed variants that were detected by exome sequencing in each sample were determined bioinformatically as likely to be presented by MHC class I molecules on AML cells at presentation, relapse, or both. Few potential neoantigens identified in this way from presentation samples were cleared at relapse (orange bars).

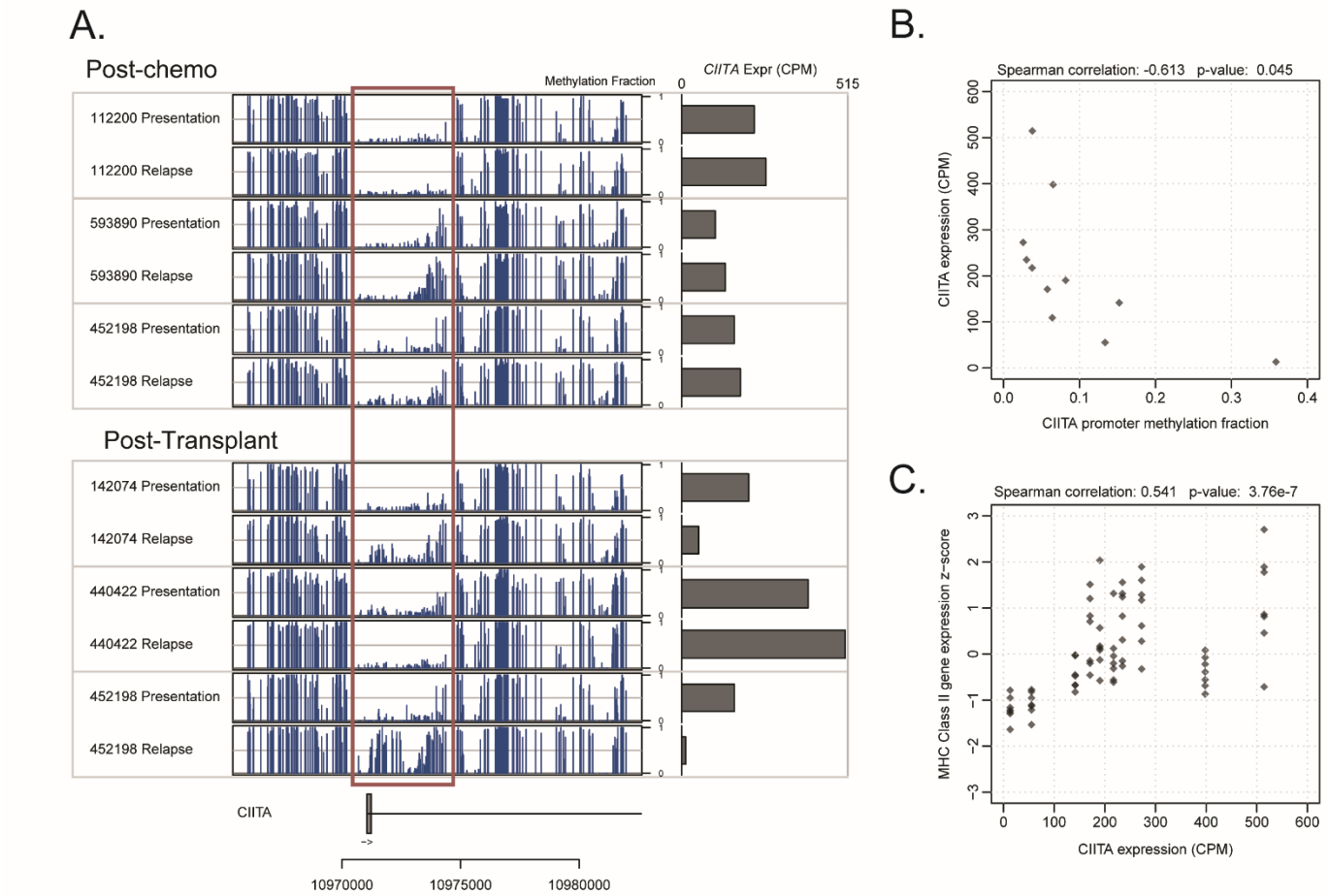

Figure S12. DNA Methylation of the *CIITA* Promotor Region in AML Samples. Matched presentation and relapse samples were obtained from post-chemotherapy (patients 112200, 593890, and 452198) and post-transplant relapse cases (patients 142074, 440422, and 452198) and DNA was subjected to whole genome bisulfite sequencing. (A) *CIITA* expression (right) and methylation of the *CIITA* promoter region in paired presentation/relapse samples from post-chemotherapy cases (top left) and post-transplant cases (bottom left). The red box shows an unmethylated region associated with the *CIITA* promoter, exon 1, and intron 1. (B) Correlation between levels of *CIITA* promoter methylation and *CIITA* gene expression. (C) Correlation between *CIITA* expression and MHC class II genes (*HLA-DPA1, HLA-DPB1, HLA-DQA1, HLA-DQB1, HLA-DRA, HLA-DRB1, HLA-DRB3*). Since these genes have substantially different expression, CPM values were converted to a "z-score" that gives a relative level of expression.

Table S1: Patient Cohort

Table 1 Clinical Data

UPN	Relapse type	FAB	Age	cytogenetic risk	Transplant type	remission status at transplant	relapse day from diagnosis	Relapse site	RNA-seq	Recurrently mutated AML genes at diagnosis
103342	after HCT	M2	61	intermediate	MUD	CR1*	1095	bone marrow	yes	*CBL, SRSF2, TET2, RUNX1, NRAS, STAG2*
142074	after HCT	M4	60	intermediate	SIB	CR1	300	bone marrow	yes	*TET2, DNMT3A, NPM1, NLRC4*
161510	after HCT	M2	44	intermediate	MUD	PD	218	bone marrow		*IDH1, WT1, PTPN11, NRAS, WT1*
242129	after HCT	M4	51	poor	MUD	CR2	403	bone marrow		MLL-ELL fusion, *SHC1, KRAS*
312451	after HCT	M2	18	intermediate	MMUD (9/10)	CR1	285	bone marrow	yes	*FLT3-ITD, NPM1*
440422	after HCT	M0	69	intermediate	MMUD (9/10)	PD	708	bone marrow	yes	*RUNX1, IDH2, SRSF2, ASXL1*
619751	after HCT	M4	57	good	MUD	CR2	493	bone marrow	yes	inv(16), *ARAP2, KIT, WT1*
814916	after HCT	M2	63	poor	MMUD (9/10)	CR1	653	bone marrow	yes	*TP53, PTPN11, SETBP1*
452198	after HCT	M4	55	intermediate	SIB	CR2	3269	bone marrow	yes	*DNMT3A, NPM1, FLT3-ITD, IDH1, FOXP1, PTPN11*
112200	after HCT	M4	43	good	SIB	CR2	2027	extramedullary		inv(16), *XIRP, NRAS*
113971	after HCT	M2	57	intermediate	MUD	CR1	711	extramedullary		*DNMT3A, TOP3B, KRAS, IDH2*
327733	after HCT	M1	32	intermediate	MUD	CR2	995	extramedullary		*IDH1, NPM1, FLT3-ITD*
593890	after HCT	M2	35	intermediate	MUD	CR2	1024	extramedullary		*CEBPA, MEFV, GATA2*
633734	after HCT	M1	53	poor	MUD	CR2	588	extramedullary		*LRP1B, SLC12A3, U2AF1, BCOR*
866660	after HCT	M2	41	intermediate	MMUD (8/10)	CR1	632	extramedullary		*GATA2, RAD21, CEBPA, NRAS*
126620	after chemo	M4	51	intermediate	--	--	84	bone marrow		*MAP1B, WT1, KRAS*
174556	after chemo	M1	65	poor	--	--	90	bone marrow		*IDH1, EZH2, RUNX1, LRP1B, PTP11*
183696	after chemo	M2	62	intermediate	--	--	300	bone marrow		*IDH1, NRAS*
196371	after chemo	M4	42	intermediate	--	--	155	bone marrow	yes	*NPM1, FLT3-TKD*
220882	after chemo	M2	71	intermediate	--	--	241	bone marrow	yes	*DNMT3A, IDH2, NRAS*
275291	after chemo	M4	54	good	--	--	278	bone marrow		INV(16), *FLT3-TKD*
286032	after chemo	M2	50	intermediate	--	--	326	bone marrow	yes	*DNMT3A, FLT3-ITD, NPM2, ZNF687*
467522	after chemo	M4	69	poor	--	--	74	bone marrow		*TET2, SRSF2*
554023	after chemo	M1	71	poor	--	--	136	bone marrow		*DNMT3A, IDH2, RUNX1, SRSF2*
695558	after chemo	M2	46	good	--	--	345	bone marrow		t(8;21)
763312	after chemo	M2	58	good	--	--	296	bone marrow		t(8;21), *JAK2, DNAH5, GATA2*
823477	after chemo	M0	51	intermediate	--	--	249	bone marrow		*U2AF1, JAK2*
875663	after chemo	M4	68	Intermediate	--	--	356	bone marrow		*DNMT3A, TET2, SF3B1, NPM1, FLT3-TKD, NRAS, SRSF2*
970171	after chemo	M2	73	poor	--	--	132	bone marrow		*TP53*
150288	after chemo	M1	51	intermediate	--	--	423	bone marrow	yes	*STAG2, PTPN11, NPM1*
303642	after chemo	M1	54	intermediate	--	--	1230	bone marrow	yes	*IDH1, GRIK2, FLT3-TKD, WT1, STAG2*
112200	after chemo	M4	43	good	--	--	865	extramedullary	yes	*XIRP, NRAS*
327733	after chemo	M1	32	intermediate	--	--	363	extramedullary	yes	*IDH1, NPM1, FLT3-ITD*
593890	after chemo	M2	35	intermediate	--	--	445	extramedullary	yes	*CEBPA, MEFV, GATA2*
452198	after chemo	M4	55	intermediate	--	--	505	bone marrow	yes	*DNMT3A, NPM1, FLT3-ITD, IDH1, FOXP1, PTPN11*

HCT, Hematopoietic Cell Transplantation; MUD, matched unrelated donor; SIB, matched sibling donor; MMUD, mismatched unrelated donor; CR, complete remission; PD, persistent disease.

Table S2: Clinical matrix
See separate Excel file:

Per-sample table containing information on disease characteristics and treatment history.

Table S3: Exome variants
See separate Excel file:

All variants discovered by enhanced exome sequencing of diagnosis and relapse samples from post-transplant and post-chemotherapy relapse groups.

Table S4: Copy number variants
See separate Excel file:

List of all copy number changes in presentation (primary) and post-relapse cases.

Table S5: Fusion transcripts

Fusion transcripts detected by RNA-sequencing in presentation (primary) and post-relapse cases.

Sample	5' gene	3' gene	Reciprocal	Splicings
112200_primary	RPL3	MPO	N	RPL3>>MPO(Inter_Chromosomal Canonical 1);
112200_post_chemo_relapse	RPL3	MPO	N	RPL3>>MPO(Inter_Chromosomal Canonical 1);
112200_post_chemo_relapse	CBFB	MYH11	N	CBFB>>MYH11(Intra_Chromosomal Canonical 6);CBFB>>MYH11(Intra_Chromosomal 18);
161510_primary	SMURF2P1	LRRC37B	N	SMURF2P1>>LRRC37B(Intra_Chromosomal Canonical 4);
161510_post_allo_relapse	SMURF2P1	LRRC37B	N	SMURF2P1>>LRRC37B(Intra_Chromosomal Canonical 4);
161510_primary	HLA-H	HLA-B	N	HLA-H>>HLA-B(Intra_Chromosomal Canonical 1);
161510_post_allo_relapse	HLA-H	HLA-B	N	HLA-H>>HLA-B(Intra_Chromosomal Canonical 1);
619751_post_allo_relapse	CBFB	MYH11	N	CBFB>>MYH11(Intra_Chromosomal Canonical 35);CBFB>>MYH11(Intra_Chromosomal Canonical 1);
619751_primary	CBFB	MYH11	N	CBFB>>MYH11(Intra_Chromosomal Canonical 16);
814916_primary	U2AF1	RUNX1	N	U2AF1>>RUNX1(Intra_Chromosomal Canonical 6);
814916_post_allo_relapse	U2AF1	RUNX1	N	U2AF1>>RUNX1(Intra_Chromosomal Canonical 6);
814916_primary	ZNF510	ZNF782	N	ZNF510>>ZNF782(Intra_Chromosomal Canonical 1);
814916_post_allo_relapse	ZNF510	ZNF782	N	ZNF510>>ZNF782(Intra_Chromosomal Canonical 1);

Table S6: RNA sequencing matrix
See separate Excel file:

Normalized RNA sequencing data from 7 post-transplant relapse and 9 post-chemo relapse cases expressed as total reads per gene.

Table S7: Differentially regulated genes

logFC = log2-fold change of expression between presentation and relapse
logCPM = average log2-counts per million
LR = log ratio statistics

<u>Upregulated at relapse</u>:

Gene	PValue	FDR	Fold Change
ADAMTS14	2.75E-08	3.97E-05	4.8
AEBP1	0.00016	0.017967	4.0
AMOTL1	2.18E-06	0.00088	2.8
ANKRD10	0.00055	0.042628	3.8
AR	0.000299	0.028435	3.6
CCDC14	0.000146	0.017047	4.1
CEP70	1.48E-05	0.003361	2.6
CPA3	0.000266	0.026583	4.1
DNAJC12	0.000522	0.041594	2.6
DPY19L2P1	0.000238	0.024298	2.8
ESYT3	3.29E-05	0.006226	5.3
FERMT1	4.27E-05	0.007454	4.1
HPGDS	0.000489	0.041204	4.8
HSPD1P11	9.78E-05	0.013399	2.9
LAPTM4B	9.93E-05	0.013488	3.3
MARCKSL1	1.10E-06	0.000548	3.3
MDFI	3.93E-05	0.007179	2.6
MEX3A	5.27E-07	0.00028	3.8
MRC2	0.000231	0.023891	3.5
PLXNB1	0.000112	0.014715	2.6
RAB38	2.36E-06	0.000915	1.9
RP11-299L17.1	0.00015	0.017231	2.7
RYR3	0.000145	0.017047	3.8
SOCS2	0.000177	0.019424	2.2
SPIN4	1.71E-05	0.003622	2.9
STON2	3.21E-05	0.006147	2.8
TMPRSS11D	5.66E-06	0.001661	2.7
TPSD1	0.000388	0.034448	4.8
TRGC1	7.54E-05	0.011098	2.6
TRGJP1	0.000132	0.01618	5.4
TRGJP2	4.38E-05	0.007571	3.5
UNGP3	7.50E-05	0.011098	2.7
WASF1	0.000227	0.023631	1.9
ZBTB10	0.000544	0.042432	1.9

Downregulated at relapse:

Gene	PValue	FDR	Fold Change
MARCH1	0.000146	0.017047	-2.3
ABI3	5.98E-06	0.001696	-5.0
AC010970.2	3.82E-08	4.05E-05	-4.2
ACPP	0.000526	0.041594	-2.9
ADAMTSL4	0.000151	0.017265	-2.2
ADAP2	2.53E-05	0.005115	-3.8
ADM	0.000504	0.041323	-3.1
AL513122.1	5.11E-05	0.008372	-21.1
ALOX5	0.000507	0.041376	-3.2
ANXA5	7.12E-06	0.001951	-8.3
AP5B1	0.000553	0.04267	-2.0
APOBR	1.68E-05	0.003622	-3.4
ARHGAP6	0.000105	0.01406	-5.2
ARHGEF10L	2.80E-07	0.000171	-27.0
BCL6	0.000514	0.041594	-4.7
C10orf105	0.000258	0.025934	-5.0
C10orf54	0.000126	0.015956	-2.7
C1orf162	1.69E-05	0.003622	-2.6
CADM1	2.21E-06	0.00088	-3.2
CAPG	0.000521	0.041594	-2.0
CCDC170	0.000536	0.042002	-3.2
CCL5	8.57E-05	0.012497	-3.1
CCR1	2.75E-06	0.001032	-5.6
CCR2	1.64E-10	1.23E-06	-9.1
CCR5	3.12E-06	0.001129	-7.2
CD14	1.07E-07	8.92E-05	-14.0
CD1D	5.79E-07	0.000297	-8.5
CD28	4.14E-05	0.007454	-5.4
CD300A	0.000329	0.030795	-2.4
CD300C	1.39E-05	0.003213	-4.6
CD300E	3.45E-12	5.49E-08	-28.1
CD300LB	8.53E-09	2.11E-05	-8.2
CD36	9.06E-05	0.012867	-4.2
CD48	0.00063	0.046144	-2.8
CD52	1.14E-05	0.002883	-2.8
CD68	0.00017	0.01878	-2.8
CD74	0.000193	0.020591	-3.2
CD86	3.10E-05	0.006004	-6.0
CHST15	8.90E-05	0.012764	-5.3
CNTNAP2	0.000225	0.023631	-3.7

COL6A3	0.000116	0.014996	-3.4
CORO1A	0.000111	0.014699	-2.2
CR1	0.000393	0.034541	-4.1
CRTAM	5.30E-05	0.008594	-3.0
CSF2RA	0.000131	0.01618	-2.6
CTSS	2.08E-06	0.000871	-2.8
CX3CR1	2.67E-07	0.00017	-12.0
DTX4	0.000131	0.01618	-4.5
EDA	0.000252	0.025473	-2.4
EEF1DP3	0.000212	0.022506	-3.1
F13A1	5.67E-05	0.009009	-3.9
FAM198B	4.87E-06	0.001581	-6.3
FAM65B	0.000276	0.027017	-2.1
FCER1G	3.67E-06	0.00124	-4.4
FCER2	4.81E-08	4.78E-05	-7.0
FCGR3A	4.92E-05	0.008231	-6.1
FGD2	1.98E-07	0.000137	-5.4
FGL2	1.36E-07	0.000103	-7.5
FGR	5.65E-06	0.001661	-6.9
FPR1	0.000292	0.028114	-3.6
FYB	0.000143	0.017047	-2.0
GIMAP1	4.71E-05	0.007969	-3.2
GIMAP4	2.47E-07	0.000163	-6.2
GIMAP7	0.000605	0.045141	-3.8
GIMAP8	0.000121	0.015408	-4.2
GLT1D1	0.000556	0.042726	-10.8
GPAT3	3.23E-08	4.05E-05	-4.0
GRM2	0.000417	0.036016	-2.3
GRN	0.000132	0.01618	-2.6
GSG1L	5.73E-09	1.82E-05	-7.7
HAVCR2	0.0005	0.041323	-2.4
HCK	3.30E-06	0.001167	-3.9
HDAC9	1.41E-06	0.00066	-3.0
HK3	1.58E-05	0.003531	-16.6
HLA-DMA	0.000611	0.045362	-2.4
HLA-DMB	4.64E-06	0.001538	-5.4
HLA-DPA1	7.28E-05	0.011018	-5.0
HLA-DPB1	5.09E-05	0.008372	-3.8
HLA-DQB1	0.000189	0.020407	-4.1
HLA-DRB1	7.41E-05	0.011098	-4.5
HLA-F	0.000572	0.043529	-2.5
HMOX1	3.35E-05	0.006267	-4.2
HSPA6	0.00016	0.017967	-4.7
HSPA7	0.000599	0.044941	-8.9

IFI30	1.99E-08	3.16E-05	-8.8
IGHA2	9.37E-05	0.013062	-4.9
IGHG2	5.15E-10	2.05E-06	-12.0
IGHG4	2.54E-05	0.005115	-10.8
IGKV2-28	2.75E-05	0.005462	-10.6
IGSF6	3.73E-05	0.006901	-3.4
IL16	0.000326	0.030687	-1.9
IPCEF1	0.000448	0.038294	-5.2
IRF8	0.000148	0.01717	-3.4
ITGAL	6.84E-08	6.40E-05	-3.4
ITGAX	1.32E-05	0.003109	-4.1
ITGB2	0.000495	0.041323	-2.5
ITGB7	0.000361	0.032787	-2.0
JAML	1.33E-05	0.003109	-8.3
KCNA3	8.16E-06	0.002161	-4.0
KCTD12	2.79E-06	0.001032	-6.0
KIAA0513	4.24E-07	0.000233	-2.9
LGALS2	1.49E-08	2.81E-05	-17.1
LGALS3	0.000141	0.016927	-6.3
LILRA1	3.69E-08	4.05E-05	-8.0
LILRB4	9.76E-05	0.013399	-6.6
LRP1	7.11E-06	0.001951	-4.3
LRRC25	0.000524	0.041594	-3.4
LRRK2	1.08E-05	0.002822	-11.0
LYZ	1.70E-05	0.003622	-12.4
MAFB	5.75E-06	0.001661	-15.0
MAST3	0.000685	0.049309	-2.4
MEFV	1.18E-05	0.002939	-2.9
MPEG1	1.59E-08	2.81E-05	-8.9
MPP3	0.000121	0.015408	-2.8
MYCL	2.33E-10	1.23E-06	-19.1
MYO1E	0.000188	0.020407	-4.0
MYO6	0.000358	0.032738	-3.1
MYOF	4.24E-05	0.007454	-7.1
NACC2	0.000456	0.038794	-3.7
NAPSB	1.29E-06	0.000622	-5.6
NCF2	0.000277	0.027017	-3.7
NEDD9	0.000294	0.028166	-2.5
NFAM1	4.98E-06	0.001585	-3.4
NLRC4	0.000497	0.041323	-3.2
NLRP1	0.00067	0.048411	-2.9
NLRP12	1.29E-05	0.003109	-4.3
NRGN	4.44E-05	0.007591	-5.8
NUAK2	0.000621	0.045715	-2.5

P2RY13	0.000336	0.031248	-4.7
PDE2A	6.39E-05	0.009864	-5.1
PECAM1	5.67E-06	0.001661	-2.3
PIK3R5	0.000226	0.023631	-2.8
PILRA	0.000388	0.034448	-2.9
PLEKHO2	0.000533	0.041957	-1.9
POU2AF1	0.000193	0.020591	-2.1
PPBP	2.16E-05	0.00446	-26.4
PSTPIP1	4.26E-05	0.007454	-3.3
PTAFR	3.58E-06	0.001237	-6.2
PTPRB	0.000409	0.035565	-2.9
RAB31	1.12E-07	8.93E-05	-9.7
RASGRP4	0.000281	0.027276	-2.3
RASSF3	0.00049	0.041204	-2.0
RBM47	8.02E-06	0.002161	-3.8
RGL1	1.99E-05	0.004166	-3.5
RNASE6	5.37E-05	0.008629	-4.9
RNF144B	2.82E-05	0.005534	-2.4
RYR1	1.33E-05	0.003109	-8.4
S100A11	0.000561	0.042885	-2.7
SAMHD1	3.38E-08	4.05E-05	-5.8
SELPLG	1.51E-06	0.000687	-2.2
SERPINA1	1.94E-06	0.000833	-11.3
SH2D3C	0.000421	0.036168	-2.1
SIGLEC9	0.000599	0.044941	-4.0
SIRPB2	1.77E-06	0.000783	-2.7
SLC11A1	0.000596	0.044941	-3.0
SLC12A1	7.13E-05	0.010907	-3.1
SLC7A7	0.000268	0.026654	-2.9
SLC8A1	0.000168	0.01868	-5.1
SORT1	8.91E-05	0.012764	-2.6
SPON1	0.000652	0.047308	-2.5
STX11	0.000234	0.024044	-3.4
SULF2	0.00035	0.032128	-2.6
SULT1A4	0.000391	0.034541	-3.5
TBC1D2	0.000517	0.041594	-2.1
TBC1D9	0.000153	0.017359	-7.0
TGFBI	3.84E-07	0.000218	-7.6
THEMIS2	0.000103	0.01391	-2.6
TLR1	0.000274	0.027009	-2.0
TLR7	5.66E-06	0.001661	-4.2
TLR8	1.79E-07	0.000129	-7.2
TMEM71	0.000504	0.041323	-1.9
TNF	0.000384	0.034448	-5.3

TNFRSF1B	6.33E-05	0.009864	-3.3
TNFSF12	1.14E-05	0.002883	-5.0
TNFSF13	0.00034	0.031457	-2.1
TNFSF8	0.000397	0.034641	-2.9
TNNI2	0.000639	0.046591	-4.6
TP53I11	9.32E-05	0.013062	-3.6
TRPS1	0.000321	0.030423	-2.4
TSHZ3	2.92E-07	0.000172	-8.0
TTC9	0.000369	0.033369	-3.4
TYROBP	8.50E-08	7.50E-05	-2.8
VCAN	9.31E-09	2.11E-05	-22.4
VIPR1	6.11E-05	0.009618	-5.0
VSIG1	0.000613	0.045362	-2.5
ZBTB47	0.000139	0.016829	-5.5
ZNF366	0.000115	0.014996	-2.9

Table S8: Functional enrichment pathway analysis
See separate Excel file:

Analysis of differentially regulated gene pathways based on Gene Ontology Consortium categories (http://geneontology.org/page/go-enrichment-analysis)

Table S9: Predicted Neoepitopes
See separate Excel file:

List of bioinformatically predicted neoepitopes present at presentation, relapse, or both in 8 cases (see Supplementary Results and Supplementary Figure 8).

Table S10: Differentially methylated regions
See separate Excel file:

Table showing differentially methylated regions discovered from whole genome bisulfite sequencing performed on 3 post-chemotherapy and 3 post-transplant relapse cases.

Table S11: Hotspot Variants Used
Table of hotspot variants used for variant filtering (see Supplementary Methods above).

chromosome	start	stop	reference	variant	type	Gene name	position	amino acid change
11	32417909	32417910	-	ACCGTACA	INS	WT1	c.1143_1142	p.A382fs
13	28592628	28592628	A	C	SNP	FLT3	c.2517	p.D839E
13	28592628	28592628	A	G	SNP	FLT3	c.2517	p.D839
13	28592628	28592628	A	T	SNP	FLT3	c.2517	p.D839E
13	28592629	28592629	T	A	SNP	FLT3	c.2516	p.D839V
13	28592629	28592629	T	C	SNP	FLT3	c.2516	p.D839G
13	28592629	28592629	T	G	SNP	FLT3	c.2516	p.D839A
13	28592630	28592630	C	A	SNP	FLT3	c.2515	p.D839Y
13	28592630	28592630	C	G	SNP	FLT3	c.2515	p.D839H
13	28592630	28592630	C	T	SNP	FLT3	c.2515	p.D839N
13	28592637	28592637	G	A	SNP	FLT3	c.2508	p.I836
13	28592637	28592637	G	C	SNP	FLT3	c.2508	p.I836M
13	28592637	28592637	G	T	SNP	FLT3	c.2508	p.I836
13	28592638	28592638	A	C	SNP	FLT3	c.2507	p.I836S
13	28592638	28592638	A	G	SNP	FLT3	c.2507	p.I836T
13	28592638	28592638	A	T	SNP	FLT3	c.2507	p.I836N
13	28592639	28592639	T	A	SNP	FLT3	c.2506	p.I836F
13	28592639	28592639	T	C	SNP	FLT3	c.2506	p.I836V
13	28592639	28592639	T	G	SNP	FLT3	c.2506	p.I836L
13	28592640	28592640	A	C	SNP	FLT3	c.2505	p.D835E
13	28592640	28592640	A	G	SNP	FLT3	c.2505	p.D835
13	28592640	28592640	A	T	SNP	FLT3	c.2505	p.D835E
13	28592641	28592641	T	A	SNP	FLT3	c.2504	p.D835V
13	28592641	28592641	T	C	SNP	FLT3	c.2504	p.D835G
13	28592641	28592641	T	G	SNP	FLT3	c.2504	p.D835A
13	28592642	28592642	C	A	SNP	FLT3	c.2503	p.D835Y
13	28592642	28592642	C	G	SNP	FLT3	c.2503	p.D835H
13	28592642	28592642	C	T	SNP	FLT3	c.2503	p.D835N
15	90631837	90631837	C	A	SNP	IDH2	c.516	p.R172S
15	90631837	90631837	C	G	SNP	IDH2	c.516	p.R172S
15	90631837	90631837	C	T	SNP	IDH2	c.516	p.R172
15	90631838	90631838	C	A	SNP	IDH2	c.515	p.R172M
15	90631838	90631838	C	G	SNP	IDH2	c.515	p.R172T
15	90631838	90631838	C	T	SNP	IDH2	c.515	p.R172K
15	90631839	90631839	T	A	SNP	IDH2	c.514	p.R172W
15	90631839	90631839	T	C	SNP	IDH2	c.514	p.R172G
15	90631839	90631839	T	G	SNP	IDH2	c.514	p.R172
15	90631933	90631933	C	A	SNP	IDH2	c.420	p.R140
15	90631933	90631933	C	G	SNP	IDH2	c.420	p.R140
15	90631933	90631933	C	T	SNP	IDH2	c.420	p.R140
15	90631934	90631934	C	A	SNP	IDH2	c.419	p.R140L
15	90631934	90631934	C	G	SNP	IDH2	c.419	p.R140P
15	90631934	90631934	C	T	SNP	IDH2	c.419	p.R140Q
15	90631935	90631935	G	A	SNP	IDH2	c.418	p.R140W
15	90631935	90631935	G	C	SNP	IDH2	c.418	p.R140G

15	90631935	90631935	G	T	SNP	IDH2	c.418	p.R140
17	7577119	7577119	A	C	SNP	TP53	c.819	p.R273
17	7577119	7577119	A	G	SNP	TP53	c.819	p.R273
17	7577119	7577119	A	T	SNP	TP53	c.819	p.R273
17	7577120	7577120	C	A	SNP	TP53	c.818	p.R273L
17	7577120	7577120	C	G	SNP	TP53	c.818	p.R273P
17	7577120	7577120	C	T	SNP	TP53	c.818	p.R273H
17	7577121	7577121	G	A	SNP	TP53	c.817	p.R273C
17	7577121	7577121	G	C	SNP	TP53	c.817	p.R273G
17	7577121	7577121	G	T	SNP	TP53	c.817	p.R273S
17	7577534	7577534	C	A	SNP	TP53	c.747	p.R249S
17	7577534	7577534	C	G	SNP	TP53	c.747	p.R249S
17	7577534	7577534	C	T	SNP	TP53	c.747	p.R249
17	7577535	7577535	C	A	SNP	TP53	c.746	p.R249M
17	7577535	7577535	C	G	SNP	TP53	c.746	p.R249T
17	7577535	7577535	C	T	SNP	TP53	c.746	p.R249K
17	7577536	7577536	T	A	SNP	TP53	c.745	p.R249W
17	7577536	7577536	T	C	SNP	TP53	c.745	p.R249G
17	7577537	7577537	C	A	SNP	TP53	c.744	p.R248
17	7577537	7577537	C	G	SNP	TP53	c.744	p.R248
17	7577537	7577537	C	T	SNP	TP53	c.744	p.R248
17	7577538	7577538	C	A	SNP	TP53	c.743	p.R248L
17	7577538	7577538	C	G	SNP	TP53	c.743	p.R248P
17	7577538	7577538	C	T	SNP	TP53	c.743	p.R248Q
17	7577539	7577539	G	A	SNP	TP53	c.742	p.R248W
17	7577539	7577539	G	C	SNP	TP53	c.742	p.R248G
17	7577539	7577539	G	T	SNP	TP53	c.742	p.R248
17	7578189	7578189	A	C	SNP	TP53	c.660	p.Y220*
17	7578189	7578189	A	G	SNP	TP53	c.660	p.Y220
17	7578189	7578189	A	T	SNP	TP53	c.660	p.Y220*
17	7578190	7578190	T	A	SNP	TP53	c.659	p.Y220F
17	7578190	7578190	T	C	SNP	TP53	c.659	p.Y220C
17	7578190	7578190	T	G	SNP	TP53	c.659	p.Y220S
17	7578191	7578191	A	C	SNP	TP53	c.658	p.Y220D
17	7578191	7578191	A	G	SNP	TP53	c.658	p.Y220H
17	7578191	7578191	A	T	SNP	TP53	c.658	p.Y220N
17	7578411	7578411	C	A	SNP	TP53	c.519	p.V173
17	7578411	7578411	C	G	SNP	TP53	c.519	p.V173
17	7578411	7578411	C	T	SNP	TP53	c.519	p.V173
17	7578412	7578412	A	C	SNP	TP53	c.518	p.V173G
17	7578412	7578412	A	G	SNP	TP53	c.518	p.V173A
17	7578412	7578412	A	T	SNP	TP53	c.518	p.V173E
17	7578413	7578413	C	A	SNP	TP53	c.517	p.V173L
17	7578413	7578413	C	G	SNP	TP53	c.517	p.V173L
17	7578413	7578413	C	T	SNP	TP53	c.517	p.V173M
1	36933433	36933433	G	A	SNP	CSF3R	c.509	p.P170L
1	36933433	36933433	G	C	SNP	CSF3R	c.509	p.P170R
1	36933433	36933433	G	T	SNP	CSF3R	c.509	p.P170H
1	36933434	36933434	G	A	SNP	CSF3R	c.1853	p.T618I
1	36933434	36933434	G	C	SNP	CSF3R	c.1853	p.T618S
1	36933434	36933434	G	T	SNP	CSF3R	c.1853	p.T618N
1	36933435	36933435	T	A	SNP	CSF3R	c.1852	p.T618S

1	36933435	36933435	T	C	SNP	CSF3R	c.1852	p.T618A
1	36933435	36933435	T	G	SNP	CSF3R	c.1852	p.T618P
21	36231781	36231781	T	A	SNP	RUNX1	c.603	p.R201
21	36231781	36231781	T	C	SNP	RUNX1	c.603	p.R201
21	36231781	36231781	T	G	SNP	RUNX1	c.603	p.R201
21	36231782	36231782	C	A	SNP	RUNX1	c.602	p.R201L
21	36231782	36231782	C	G	SNP	RUNX1	c.602	p.R201P
21	36231782	36231782	C	T	SNP	RUNX1	c.602	p.R201Q
21	36231783	36231783	G	A	SNP	RUNX1	c.601	p.R201*
21	36231783	36231783	G	C	SNP	RUNX1	c.601	p.R201G
21	36231783	36231783	G	T	SNP	RUNX1	c.601	p.R201
21	36252876	36252876	C	A	SNP	RUNX1	c.486	p.R162S
21	36252876	36252876	C	G	SNP	RUNX1	c.486	p.R162S
21	36252876	36252876	C	T	SNP	RUNX1	c.486	p.R162
21	36252877	36252877	C	A	SNP	RUNX1	c.485	p.R162M
21	36252877	36252877	C	G	SNP	RUNX1	c.485	p.R162T
21	36252877	36252877	C	T	SNP	RUNX1	c.485	p.R162K
21	36252878	36252878	T	A	SNP	RUNX1	c.484	p.R162W
21	36252878	36252878	T	C	SNP	RUNX1	c.484	p.R162G
21	36252878	36252878	T	G	SNP	RUNX1	c.484	p.R162
21	44514776	44514776	C	A	SNP	U2AF1	c.471	p.Q157H
21	44514776	44514776	C	G	SNP	U2AF1	c.471	p.Q157H
21	44514776	44514776	C	T	SNP	U2AF1	c.471	p.Q157
21	44514777	44514777	T	A	SNP	U2AF1	c.470	p.Q157L
21	44514777	44514777	T	C	SNP	U2AF1	c.470	p.Q157R
21	44514777	44514777	T	G	SNP	U2AF1	c.470	p.Q157P
21	44514778	44514778	G	A	SNP	U2AF1	c.469	p.Q157*
21	44514778	44514778	G	C	SNP	U2AF1	c.469	p.Q157E
21	44514778	44514778	G	T	SNP	U2AF1	c.469	p.Q157K
21	44524455	44524455	A	C	SNP	U2AF1	c.102	p.S34
21	44524455	44524455	A	G	SNP	U2AF1	c.102	p.S34
21	44524455	44524455	A	T	SNP	U2AF1	c.102	p.S34
21	44524456	44524456	G	A	SNP	U2AF1	c.101	p.S34F
21	44524456	44524456	G	C	SNP	U2AF1	c.101	p.S34C
21	44524456	44524456	G	T	SNP	U2AF1	c.101	p.S34Y
21	44524457	44524457	A	C	SNP	U2AF1	c.100	p.S34A
21	44524457	44524457	A	G	SNP	U2AF1	c.100	p.S34P
21	44524457	44524457	A	T	SNP	U2AF1	c.100	p.S34T
2	198266832	198266832	T	A	SNP	SF3B1	c.2100	p.K700N
2	198266832	198266832	T	C	SNP	SF3B1	c.2100	p.K700
2	198266832	198266832	T	G	SNP	SF3B1	c.2100	p.K700N
2	198266833	198266833	T	A	SNP	SF3B1	c.2099	p.K700I
2	198266833	198266833	T	C	SNP	SF3B1	c.2099	p.K700R
2	198266833	198266833	T	G	SNP	SF3B1	c.2099	p.K700T
2	198266834	198266834	T	A	SNP	SF3B1	c.2098	p.K700*
2	198266834	198266834	T	C	SNP	SF3B1	c.2098	p.K700E
2	198266834	198266834	T	G	SNP	SF3B1	c.2098	p.K700Q
2	198267359	198267359	C	A	SNP	SF3B1	c.1998	p.K666N
2	198267359	198267359	C	G	SNP	SF3B1	c.1998	p.K666N
2	198267359	198267359	C	T	SNP	SF3B1	c.1998	p.K666
2	198267360	198267360	T	A	SNP	SF3B1	c.1997	p.K666M
2	198267360	198267360	T	C	SNP	SF3B1	c.1997	p.K666R

2	198267360	198267360	T	G	SNP	SF3B1	c.1997	p.K666T
2	198267361	198267361	T	A	SNP	SF3B1	c.1996	p.K666*
2	198267361	198267361	T	C	SNP	SF3B1	c.1996	p.K666E
2	198267361	198267361	T	G	SNP	SF3B1	c.1996	p.K666Q
2	209113111	209113111	A	C	SNP	IDH1	c.396	p.R132
2	209113111	209113111	A	G	SNP	IDH1	c.396	p.R132
2	209113111	209113111	A	T	SNP	IDH1	c.396	p.R132
2	209113112	209113112	C	A	SNP	IDH1	c.395	p.R132L
2	209113112	209113112	C	G	SNP	IDH1	c.395	p.R132P
2	209113112	209113112	C	T	SNP	IDH1	c.395	p.R132H
2	209113113	209113113	G	A	SNP	IDH1	c.394	p.R132C
2	209113113	209113113	G	C	SNP	IDH1	c.394	p.R132G
2	209113113	209113113	G	T	SNP	IDH1	c.394	p.R132S
2	25457241	25457241	G	A	SNP	DNMT3A	c.2646	p.R882
2	25457241	25457241	G	C	SNP	DNMT3A	c.2646	p.R882
2	25457241	25457241	G	T	SNP	DNMT3A	c.2646	p.R882
2	25457242	25457242	C	A	SNP	DNMT3A	c.2645	p.R882L
2	25457242	25457242	C	G	SNP	DNMT3A	c.2645	p.R882P
2	25457242	25457242	C	T	SNP	DNMT3A	c.2645	p.R882H
2	25457243	25457243	G	A	SNP	DNMT3A	c.2644	p.R882C
2	25457243	25457243	G	C	SNP	DNMT3A	c.2644	p.R882G
2	25457243	25457243	G	T	SNP	DNMT3A	c.2644	p.R882S
3	128200111	128200111	C	A	SNP	GATA2	c.1194	p.R398
3	128200111	128200111	C	G	SNP	GATA2	c.1194	p.R398
3	128200111	128200111	C	T	SNP	GATA2	c.1194	p.R398
3	128200112	128200112	C	A	SNP	GATA2	c.1193	p.R398L
3	128200112	128200112	C	G	SNP	GATA2	c.1193	p.R398P
3	128200112	128200112	C	T	SNP	GATA2	c.1193	p.R398Q
3	128200113	128200113	G	A	SNP	GATA2	c.1192	p.R398W
3	128200113	128200113	G	C	SNP	GATA2	c.1192	p.R398G
3	128200113	128200113	G	T	SNP	GATA2	c.1192	p.R398
3	128200743	128200743	C	A	SNP	GATA2	c.1062	p.T354
3	128200743	128200743	C	G	SNP	GATA2	c.1062	p.T354
3	128200743	128200743	C	T	SNP	GATA2	c.1062	p.T354
3	128200744	128200744	G	A	SNP	GATA2	c.1061	p.T354M
3	128200744	128200744	G	C	SNP	GATA2	c.1061	p.T354R
3	128200744	128200744	G	T	SNP	GATA2	c.1061	p.T354K
3	128200745	128200745	T	A	SNP	GATA2	c.1060	p.T354S
3	128200745	128200745	T	C	SNP	GATA2	c.1060	p.T354A
3	128200745	128200745	T	G	SNP	GATA2	c.1060	p.T354P
4	55599322	55599322	T	A	SNP	KIT	c.2448	p.D816E
4	55599322	55599322	T	C	SNP	KIT	c.2448	p.D816
4	55599322	55599322	T	G	SNP	KIT	c.2448	p.D816E
5	170837546	170837547	-	CATG	INS	NPM1	c.862_863	p.W288fs
5	170837546	170837547	-	CCTG	INS	NPM1	c.862_863	p.W288fs
5	170837546	170837547	-	TCAG	INS	NPM1	c.862_863	p.W288fs
5	170837546	170837547	-	TCTG	INS	NPM1	c.862_863	p.W288fs
9	5073770	5073770	G	A	SNP	JAK2	c.1849	p.V617I
9	5073770	5073770	G	C	SNP	JAK2	c.1849	p.V617L
9	5073770	5073770	G	T	SNP	JAK2	c.1849	p.V617F
9	5073771	5073771	T	A	SNP	JAK2	c.1850	p.V617D
9	5073771	5073771	T	C	SNP	JAK2	c.1850	p.V617A

9	5073771	5073771	T	G	SNP	JAK2	c.1850	p.V617G
9	5073772	5073772	C	A	SNP	JAK2	c.1851	p.V617
9	5073772	5073772	C	G	SNP	JAK2	c.1851	p.V617
9	5073772	5073772	C	T	SNP	JAK2	c.1851	p.V617
12	25378560	25378560	T	A	SNP	KRAS	c.438	p.A146
12	25378560	25378560	T	C	SNP	KRAS	c.438	p.A146
12	25378560	25378560	T	G	SNP	KRAS	c.438	p.A146
12	25378561	25378561	G	A	SNP	KRAS	c.437	p.A146V
12	25378561	25378561	G	C	SNP	KRAS	c.437	p.A146G
12	25378561	25378561	G	T	SNP	KRAS	c.437	p.A146E
12	25378562	25378562	C	A	SNP	KRAS	c.436	p.A146S
12	25378562	25378562	C	G	SNP	KRAS	c.436	p.A146P
12	25378562	25378562	C	T	SNP	KRAS	c.436	p.A146T
12	25378647	25378647	T	A	SNP	KRAS	c.351	p.K117N
12	25378647	25378647	T	C	SNP	KRAS	c.351	p.K117
12	25378647	25378647	T	G	SNP	KRAS	c.351	p.K117N
12	25378648	25378648	T	A	SNP	KRAS	c.350	p.K117I
12	25378648	25378648	T	C	SNP	KRAS	c.350	p.K117R
12	25378648	25378648	T	G	SNP	KRAS	c.350	p.K117T
12	25378649	25378649	T	A	SNP	KRAS	c.349	p.K117*
12	25378649	25378649	T	C	SNP	KRAS	c.349	p.K117E
12	25378649	25378649	T	G	SNP	KRAS	c.349	p.K117Q
12	25380275	25380275	T	A	SNP	KRAS	c.183	p.Q61H
12	25380275	25380275	T	C	SNP	KRAS	c.183	p.Q61
12	25380275	25380275	T	G	SNP	KRAS	c.183	p.Q61H
12	25380276	25380276	T	A	SNP	KRAS	c.182	p.Q61L
12	25380276	25380276	T	C	SNP	KRAS	c.182	p.Q61R
12	25380276	25380276	T	G	SNP	KRAS	c.182	p.Q61P
12	25380277	25380277	G	A	SNP	KRAS	c.181	p.Q61*
12	25380277	25380277	G	C	SNP	KRAS	c.181	p.Q61E
12	25380277	25380277	G	T	SNP	KRAS	c.181	p.Q61K
12	25398280	25398280	G	A	SNP	KRAS	c.39	p.G13
12	25398280	25398280	G	C	SNP	KRAS	c.39	p.G13
12	25398280	25398280	G	T	SNP	KRAS	c.39	p.G13
12	25398281	25398281	C	A	SNP	KRAS	c.38	p.G13V
12	25398281	25398281	C	G	SNP	KRAS	c.38	p.G13A
12	25398281	25398281	C	T	SNP	KRAS	c.38	p.G13D
12	25398282	25398282	C	A	SNP	KRAS	c.37	p.G13C
12	25398282	25398282	C	G	SNP	KRAS	c.37	p.G13R
12	25398282	25398282	C	T	SNP	KRAS	c.37	p.G13S
12	25398283	25398283	A	C	SNP	KRAS	c.36	p.G12
12	25398283	25398283	A	G	SNP	KRAS	c.36	p.G12
12	25398283	25398283	A	T	SNP	KRAS	c.36	p.G12
12	25398284	25398284	C	A	SNP	KRAS	c.35	p.G12V
12	25398284	25398284	C	G	SNP	KRAS	c.35	p.G12A
12	25398284	25398284	C	T	SNP	KRAS	c.35	p.G12D
12	25398285	25398285	C	A	SNP	KRAS	c.34	p.G12C
12	25398285	25398285	C	G	SNP	KRAS	c.34	p.G12R
12	25398285	25398285	C	T	SNP	KRAS	c.34	p.G12S
1	115256528	115256528	T	A	SNP	NRAS	c.183	p.Q61H
1	115256528	115256528	T	C	SNP	NRAS	c.183	p.Q61
1	115256528	115256528	T	G	SNP	NRAS	c.183	p.Q61H

1	115256529	115256529	T	A	SNP	NRAS	c.182	p.Q61L
1	115256529	115256529	T	C	SNP	NRAS	c.182	p.Q61R
1	115256529	115256529	T	G	SNP	NRAS	c.182	p.Q61P
1	115256530	115256530	G	A	SNP	NRAS	c.181	p.Q61*
1	115256530	115256530	G	C	SNP	NRAS	c.181	p.Q61E
1	115256530	115256530	G	T	SNP	NRAS	c.181	p.Q61K
1	115258743	115258743	A	C	SNP	NRAS	c.39	p.G13
1	115258743	115258743	A	G	SNP	NRAS	c.39	p.G13
1	115258743	115258743	A	T	SNP	NRAS	c.39	p.G13
1	115258744	115258744	C	A	SNP	NRAS	c.38	p.G13V
1	115258744	115258744	C	G	SNP	NRAS	c.38	p.G13A
1	115258744	115258744	C	T	SNP	NRAS	c.38	p.G13D
1	115258745	115258745	C	A	SNP	NRAS	c.37	p.G13C
1	115258745	115258745	C	G	SNP	NRAS	c.37	p.G13R
1	115258745	115258745	C	T	SNP	NRAS	c.37	p.G13S
1	115258746	115258746	A	C	SNP	NRAS	c.36	p.G12
1	115258746	115258746	A	G	SNP	NRAS	c.36	p.G12
1	115258746	115258746	A	T	SNP	NRAS	c.36	p.G12
1	115258747	115258747	C	A	SNP	NRAS	c.35	p.G12V
1	115258747	115258747	C	G	SNP	NRAS	c.35	p.G12A
1	115258747	115258747	C	T	SNP	NRAS	c.35	p.G12D
1	115258748	115258748	C	A	SNP	NRAS	c.34	p.G12C
1	115258748	115258748	C	G	SNP	NRAS	c.34	p.G12R
1	115258748	115258748	C	T	SNP	NRAS	c.34	p.G12S
7	140453135	140453135	C	T	SNP	BRAF	c.1800	p.V600
7	140453136	140453136	A	C	SNP	BRAF	c.1799	p.V600G
7	140453136	140453136	A	G	SNP	BRAF	c.1799	p.V600A
7	140453136	140453136	A	T	SNP	BRAF	c.1799	p.V600E
7	140453137	140453137	C	A	SNP	BRAF	c.1798	p.V600L
7	140453137	140453137	C	G	SNP	BRAF	c.1798	p.V600L
7	140453137	140453137	C	T	SNP	BRAF	c.1798	p.V600M
9	5073770	5073770	G	A	SNP	JAK2	c.1849	p.V617I
9	5073770	5073770	G	C	SNP	JAK2	c.1849	p.V617L
9	5073770	5073770	G	T	SNP	JAK2	c.1849	p.V617F
9	5073771	5073771	T	A	SNP	JAK2	c.1850	p.V617D
9	5073771	5073771	T	C	SNP	JAK2	c.1850	p.V617A
9	5073771	5073771	T	G	SNP	JAK2	c.1850	p.V617G
9	5073772	5073772	C	A	SNP	JAK2	c.1851	p.V617
9	5073772	5073772	C	G	SNP	JAK2	c.1851	p.V617
9	5073772	5073772	C	T	SNP	JAK2	c.1851	p.V617
9	5078360	5078360	A	C	SNP	JAK2	c.2047	p.R683
9	5078360	5078360	A	G	SNP	JAK2	c.2047	p.R683G
9	5078360	5078360	A	T	SNP	JAK2	c.2047	p.R683*
9	5078361	5078361	G	A	SNP	JAK2	c.2048	p.R683K
9	5078361	5078361	G	C	SNP	JAK2	c.2048	p.R683T
9	5078361	5078361	G	T	SNP	JAK2	c.2048	p.R683I
9	5078362	5078362	A	C	SNP	JAK2	c.2049	p.R683S
9	5078362	5078362	A	G	SNP	JAK2	c.2049	p.R683
9	5078362	5078362	A	T	SNP	JAK2	c.2049	p.R683S